Comparative Analysis of Traditional Recurrent Neural Networks and Reservoir Computing Models for Predicting Complex Ball Trajectories in a 2D Environment

Minerva University

Nikita Koloskov
April 2023

Complimentary Github Repository: https://github.com/Carterochka/capstone

Title: Comparative Analysis of Traditional Recurrent Neural Networks and Reservoir Computing Models for Predicting Complex Ball Trajectories in a 2D Environment.
Author: Nikita Koloskov (Minerva University, Class of 2023).

Problem & Background:
I am exploring the use of recurrent neural networks (RNNs) to learn underlying physics in classical mechanics scenarios, specifically predicting the trajectories of single ball objects in 2D physics simulations. I am using the Phyre simulator to generate data and isolate the intuitive physics problem from contextual inference. My research is motivated by potential uses in various fields, such as robotics, the military, neuroscience, and general AI. My capstone discusses how RNNs can be leveraged to understand the underlying physics of classical mechanics scenarios by attempting to learn Newton's Laws of Motion and the Law of Conservation of Momentum. I am using the analysis of how well RNNs can predict trajectories as a proxy for speculating how accurately the models learn these laws of Physics.

Approaches:
I am using a bottom-up research approach. I started with using simple Feedforward Neural Networks to predict one time-step at a time in free-fall scenarios, using input that allows solving the same problem analytically. I am then transitioning to predicting the whole free-fall and bounce in a single-dimension scenario by using only the initial state as an input. Step by step I am increasing the complexity of the problem: by including the second coordinate, then including two other balls to the input, transitioning to scenarios with falls and collisions, and finally predicting the evolution of the entire scene with three balls. I am comparing the performance of Recurrent Neural Networks models (among which are Vanilla RNN, GRU, and LSTM) to that of Reservoir Computing (RC) models (among which are Echo State Networks and their deep variations) on each of the tasks mentioned above.

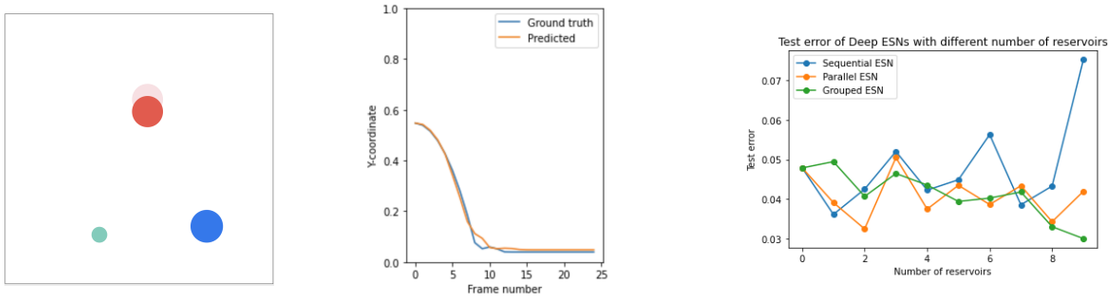

Figure 1. (left) Visual output from Phyre physics simulator; (middle) Predicted and ground truth red ball's Y-coordinate time-series in free-fall; (right) Test set performance of Deep ESN models as a function of the number of reservoirs.

Outcomes:
Traditional RNN architectures demonstrated outperformed RC models on each of the explored tasks. All models demonstrated a solid ability to predict the trajectory of the ball in the scenarios where it free-falls and bounces from the ground, but struggled to provide reasonable predictions in scenarios where it collided with other balls. Arguably, RC models demonstrate a better grasp of the underlying physics while struggling with the precision of predicted values. It especially manifests in the shape of predicted trajectories for the free-fall scenarios: RC models correctly predicted the fall strictly along a straight line, as well as the bounce once the ball hits the ground. In contrast, traditional RNNs do not grasp such aspects, but the free-fall trajectories are predicted with a much smaller error. For scenarios with collisions, both types of models fail to accurately predict the trajectories. RC models tend to fail to correctly identify collisions but somewhat reasonably predict the movement after collisions that are identified incorrectly. Traditional RNNs, in contrast, tend to fail to identify the movement correctly but are doing a better job minimizing the overall error.

Table of contents

Section 1. Introduction

In this project, I investigate the potential of recurrent neural networks (RNNs) in learning the underlying principles of classical mechanics, specifically focusing on trajectory predictions in two-dimensional (2D) physics simulations. My research is centered on predicting the trajectories of single ball objects within scenes containing no more than three ball objects, allowing for a more in-depth exploration of the subject. To generate the data, I utilize the Phyre simulator, an unlimited data source that enables me to isolate the intuitive physics problem from contextual inference.

My research is motivated by numerous potential applications across various disciplines, such as robotics, military, neuroscience, and general artificial intelligence (AI). In the field of robotics, understanding the physical dynamics of objects and predicting their trajectories can enhance the analysis of physical interventions' impacts. Similarly, in military applications, the ability to predict artillery or missile parts' trajectories post-impact could prove invaluable for devising defense tactics. Furthermore, modeling the human brain's perception of object dynamics could benefit neuroscience research and general AI tasks, including the modeling of environmental perception.

In this paper, I will discuss the implications of my research and the potential of leveraging neural networks to comprehend the underlying physics of classical mechanics scenarios. Accurate trajectory prediction requires the proper application of Newton's Laws of Motion and the Law of Conservation of Momentum. Analyzing the RNNs' performance in predicting object trajectories can serve as a proxy for determining the extent to which these models learn and apply the aforementioned laws of Physics.

Section 2. Previous Work

In this research paper, I investigate the application of Recurrent Neural Network (RNN) and Echo State Network (ESN) architectures in predicting object trajectories within simulated classical mechanics scenarios. This study builds upon prior work exploring deep learning techniques in image understanding, trajectory, and destination prediction.

Mottaghi et al. (2015) proposed a novel framework for Newtonian image understanding, analyzing static images by modeling the dynamics of objects within them. Their approach employed a Convolutional Neural Network (CNN) to learn object features and a physics-based model to predict each object's future state. Despite the model's efficacy in predicting object trajectories in images, it was limited by the reliance on only 12 modeled trajectories and did not consider object interactions beyond interactions with the ground.

In a subsequent study, Mottaghi et al. (2016) explored predicting the impact of external forces on objects in images. Their framework combined deep learning with physics-based models, learning a representation of the object and force before predicting the object's future state post-force application. The authors showed that their approach achieved state-of-the-art results on several datasets, including real-world images. However, their trajectory prediction was limited to the binary prediction about whether the object can move along a specified direction and by how much.

In Song et al.'s (2020) work on destination prediction, the authors proposed using a Deep Echo State Network (DeepESN) to predict the destination of an object based on its trajectory. DeepESN is a variant of the popular Echo State Network (ESN) that is capable of learning complex temporal dynamics. The authors showed that their model outperformed several baselines on a dataset of taxi trajectories, demonstrating its potential for applications such as traffic prediction. The moving space of the considered problem, however, is a city rather than a classical mechanics environment. So instead of being a problem of intuitive physics, it is a problem of modeling human decisions.

Finally, Wu et al. (2017) proposed a recurrent neural network (RNN) based approach for modeling trajectories. Their method uses a variant of RNN called Long Short-Term Memory

(LSTM) to capture long-term dependencies in the trajectory data. The authors evaluated their model on several datasets, including human motion tracking and vehicle navigation, and showed that it outperformed several previous methods. Despite outperforming previous methods in human motion tracking and vehicle navigation, however, their focus remained on modeling human behavior rather than intuitive physics.

In summary, previous works demonstrate deep learning techniques' potential in various tasks related to image understanding, trajectory, and destination prediction. These methods have proven accurate and applicable in real-world scenarios, such as traffic prediction and human motion tracking. My research aims to explore the capabilities of recurrent neural networks in predicting trajectories within deterministic physics-based scenarios.

Section 3. Data Preparation

To generate data for this study, I am utilizing the simulator provided by the Phyre benchmark package (Bakhtin et al., 2019). I am adapting the generated data to a format compatible with the PyTorch Deep Learning framework (Paszke et al., 2019).

3.1. Overview of the simulator

The Phyre benchmark (Bakhtin et al., 2019) offers a two-dimensional simulated environment with Newtonian physics and a set of tasks for evaluating Intuitive Physics algorithms. Each task's initial state contains a varying number of geometric bodies, distinguishable by shape and color. Users can place one or two additional red balls in the scene, depending on the task tier, with customizable location and radius. Phyre can then simulate the scenario according to programmed physics.

Upon completing the simulation, Phyre provides two output types: visual (a set of graphical data representing the simulation state at each step) and numerical (a tensor containing information about each object in the scene at every simulation step). In the numerical output, each object is characterized by 14 values as described in Bakhtin et al. (2019) supporting Jupyter Notebook:

- x- and y-coordinates of the center of mass in pixels, divided by scene width and height, respectively;
- Object orientation (angle) in radians, divided by 2π;
- Object diameter in pixels, divided by scene width;
- One-hot encoding of object shape, in the order of "ball," "bar," "jar," "standing sticks";
- One-hot encoding of object color, in the order of "red," "green," "blue," "purple," "gray," "black."

An example of the visual output is provided in Figure 1 (a), and an example of the numerical output for the initial state of the scenario is shown in Figure 1 (b).

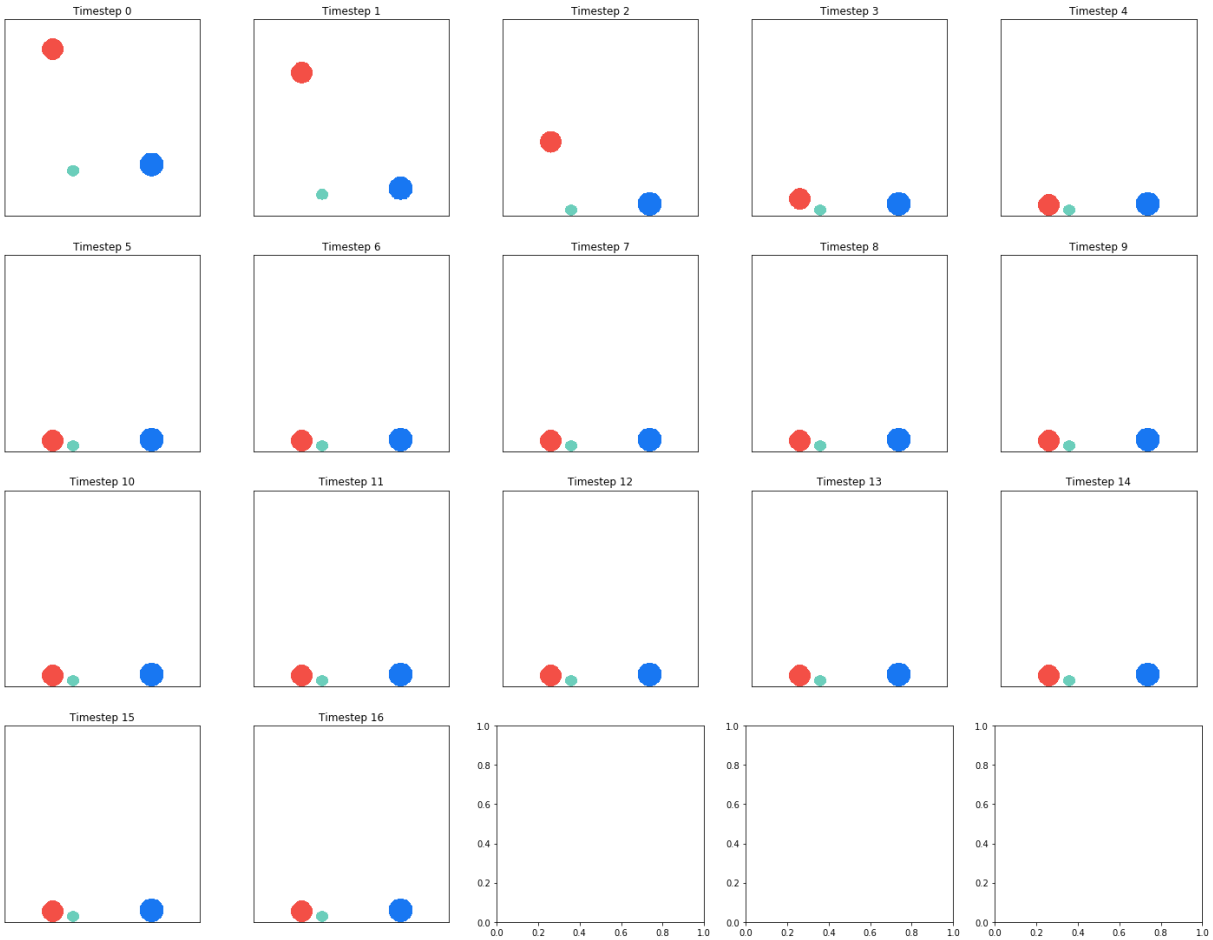

(a)

```
Initial featurized objects shape=(1, 2, 14) dtype=float32
[[[0.35  0.229 0.    0.059 1.    0.    0.    0.    0.    1.    0.
   0.    0.    0.   ]
  [0.75  0.261 0.    0.121 1.    0.    0.    0.    0.    0.    1.
   0.    0.    0.   ]]]
```

(b)

Figure 1. Graphical output of the sample simulation (a) and numerical output for the initial state (b) of the Phyre simulator. Retrieved from https://github.com/facebookresearch/phyre/blob/main/examples/01_phyre_intro.ipynb

Phyre provides a set of templates containing objects with different topologies. Each template contains a set of similar tasks with objects arranged differently in the initial state. While using the simulator, users have the ability to choose a template, task, action (where to put the ball(s) and how big to make them), and the simulation stride (how big is the gap between two simulation steps).

3.2. Preparation of the datasets

For my research project, I am focusing on scenarios with three balls, aiming to predict the trajectory of the red ball. I will use the simulator's numerical output, which allows me to separate the problem of learning physics from the problem of inferring information from visual data. The only information I will need to retrieve from the simulator is the x- and y-coordinates of each ball and their diameters. I will also use the visual output from the simulator, but solely for visualization purposes.

To generate data that only contains three balls in each scene, I am restricting my dataset to the Phyre template with the code name `'00000'`, tasks from which can be seen in the demo playground that supports Bakhtin et. al. (2019) paper. For each task in this template, I am randomly sampling actions – triplets of x- and y-coordinates and the diameter of the red ball. I use the simulator's functionality to filter out invalid simulations, such as when parts of the red ball fall outside the simulator space or overlap with other balls. The remaining simulations are further processed for each specific type of task explored in my research.

To make my data easily usable with the PyTorch framework, I need to wrap it using the PyTorch `Dataset` class. I created an abstract `ClassicalMechanicsDataset` class that extends the abstract PyTorch `Dataset`. This abstract class serves as an umbrella data class for all my research, and provides the following functionality:

- It defines an abstract method `generate_data()` that must be implemented by the child classes. In child classes, this method invokes the Phyre simulator for simulated scenarios, each of which will be stored in a separate file.
- This class implements a static function `train_test_split(path, test_frac)` that takes the path to raw data files and test fraction as input, and outputs train and test

dataset objects. This method can create dataset objects of child classes, so it doesn't need to be reimplemented during inheritance.

- It implements the `__len__(self)` method that is required by the abstract `Dataset` class by counting the number of stored data files corresponding to the given `ClassicalMechanicsDataset` instance.

For each research task that I have in the process, I extend `ClassicalMechanicsDataset` and implement the `generate_data()` method, as well as the `__getitem__(self, idx)` method required by the abstract PyTorch `Dataset` class.

Section 4. Free-fall analysis

I begin my research by exploring how machine learning models can predict the simplest type of trajectories, such as the trajectory of an object in free-fall. While the free-fall motion can be analytically calculated using kinematic equations and does not require machine learning techniques, I introduce additional complexity by focusing on the motion of a free-falling ball that hits the ground and bounces. This task is more challenging because such a trajectory cannot be described with a single mathematical equation. Furthermore, as illustrated in Figure 2, the bounce is not fully elastic, introducing a hidden physics parameter that machine learning models will need to infer: the coefficient of restitution.

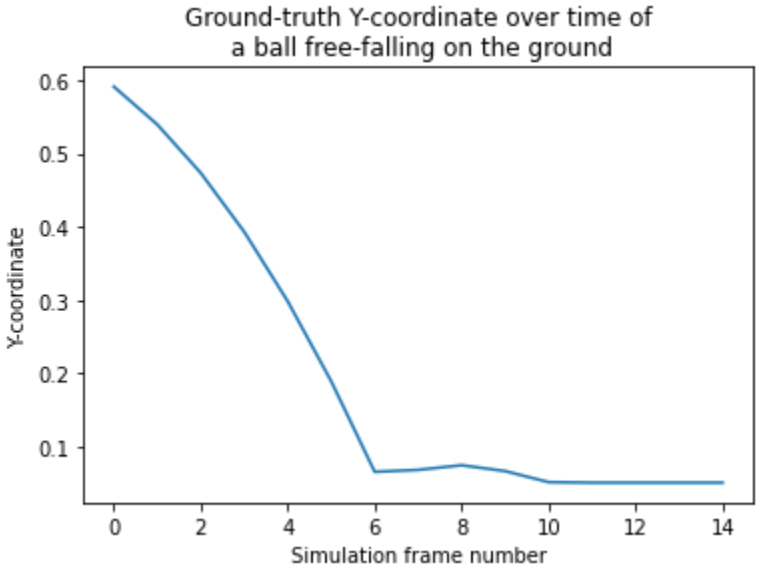

Figure 2. Simulated Y-coordinate of a ball free-falling on the ground. In case of a completely elastic collision, the ball would bounce to the initial height level.

4.1. Experiments with Feedforward Neural Networks

I begin with a naïve approach, using a feedforward neural network (FNN) as the first model to investigate patterns in the generated data. This choice is motivated by two main considerations: (1) the ability of FNNs to identify complex patterns in data, and (2) their relative ease of implementation. However, this approach is considered naïve because FNNs lack the ability to

model temporal dependencies, which are essential for predicting trajectories in time series data. As a result, FNNs may struggle to capture the dynamics of the ball's motion accurately. Despite this limitation, an analysis of the results obtained with FNNs could potentially guide further research directions and serve as a reference point to compare the performance of more complex models that can better handle time-dependent data.

4.1.1. Predicting one step at a time

While I increased the complexity of the problem by adding the bounce to the ball's trajectory, I decided to start by exploring how well linear networks can learn simple kinematic equations.

Movement of the object along a straight line can be described with the following equation:

$$\vec{r} = \vec{r}_0 + \vec{v}_0 \Delta t + \frac{1}{2}\vec{a}(\Delta t)^2 \qquad (1),$$

where $\vec{r}$ and $\vec{r}_0$ represent current and initial positions respectively, $\vec{v}_0$ is initial velocity, $\vec{a}$ is acceleration, and Δt is the time of movement. In the case of the free-fall due to gravity, when the movement is strictly vertical, assuming the direction of vertical Y-axis upwards and the direction of initial velocity downwards (which is the case for the free-fall if the movement doesn't start from rest), this equation can be rewritten as

$$y = y_0 - v_0 \Delta t - \frac{1}{2} g(\Delta t)^2 \qquad (2),$$

Equation 2 gives us the relationship between initial coordinate y_0, initial vertical velocity v_0, acceleration due to gravity g, and time step Δt. We can simplify this equation in the following way:

- Given that our simulation is discrete, Δt is defined to be one simulation frame. This simplification removes time dependency from equation 2.
- Let y_0 be the coordinate of the object on the current frame, and y be the coordinate of the object on the following frame. Then, v_0 is the velocity of the object on the current frame. In such framing, we treat each frame as initial for calculating the following frame.

- Vertical velocity is the first derivative of the y-coordinate. Given the discretized time, and assuming there was some movement preceding the current frame, it can be expressed using the equation of numerical differentiation:

$$v_0 \approx \frac{y_0 - y_{-1}}{\Delta t} = y_0 - y_{-1}.$$

  This simplifies the dependency of the following coordinate on speed in equation 2 to the dependency on coordinates on two subsequent preceding frames.

- Acceleration is the first derivative of velocity. We can use the same trick as above to get:

$$g \approx \frac{v_0 - v_{-1}}{\Delta t} = v_0 - v_{-1}.$$

  We already expressed v_0 in terms of two subsequent coordinates. In the same way,

$$v_{-1} \approx y_{-1} - y_{-2},$$

  which brings us to

$$g \approx y_0 - 2y_{-1} + y_{-2}$$

  This simplifies the dependency of the following coordinate on acceleration due gravity in equation 2 to the dependency on coordinates on three preceding frames.

So equation 2 simplifies to the equation of the form

$$y \approx f(y_0, y_{-1}, y_{-2}).$$

It means that knowing the coordinates on the three preceding frames is enough to predict the coordinate on the next frame. The purpose of the neural network will be to learn this function f. In fact, making the substitution of the equations above to 2 will give us the analytical form of f, so I expect the neural network to learn it without problems. As a result, I expect the linear network to make a close-to-perfect prediction of the next coordinate on a free-fall part of the ball movement and have a noticeable prediction error for the bounce part.

The neural network design can be inspired by the discussion above. The size of the input layer is 3, which corresponds to three subsequent coordinates. The hidden layer has 2 neurons, which are supposed to represent speed and acceleration. Finally, the dimensionality of the output is 1, which corresponds to the predicted following coordinate.

For this scenario, I generated a dataset of 5,360 simulations, 1,608 of which were used as a test set. To generate this dataset, I randomly sampled 10,000 actions[1]. Using Phyre functionality, I filtered the invalid simulations, and then implemented another filter that only leaves the simulations where the x-coordinate of the ball stays constant. Finally, I transformed each simulation into a set of 16 triplets of coordinates of a single free-falling ball, representing the position of the ball on the three consecutive simulation frames.

I implemented 3 different variations of this simple network that I trained and tested using the simulated data. The base model is a feedforward network with a single two-neuron hidden layer followed by the ReLU activation. The second model uses ReLU activation for one of the hidden neurons and cotangent activation for the second one to account for velocity being able to take different signs. Finally, the third one uses ReLU activations for both hidden neurons but also includes a direct connection from one of the input neurons to the output. Schematically, all three models are shown in Figure 3.

To quantify the model performance, I used Root Mean Squared Error (RMSE) loss.

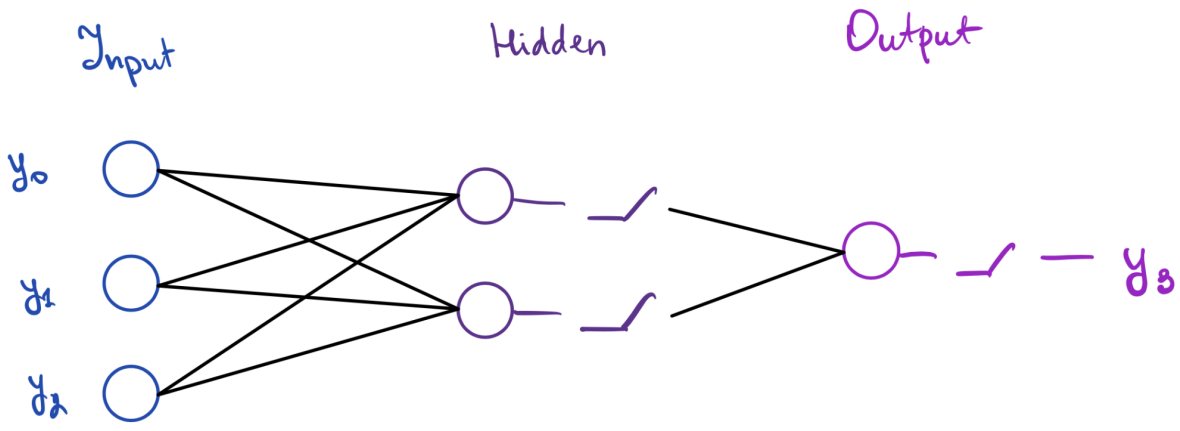

(a)

[1] Here, action is defined as a triplet of x- and y-coordinates and the diameter of the target ball.

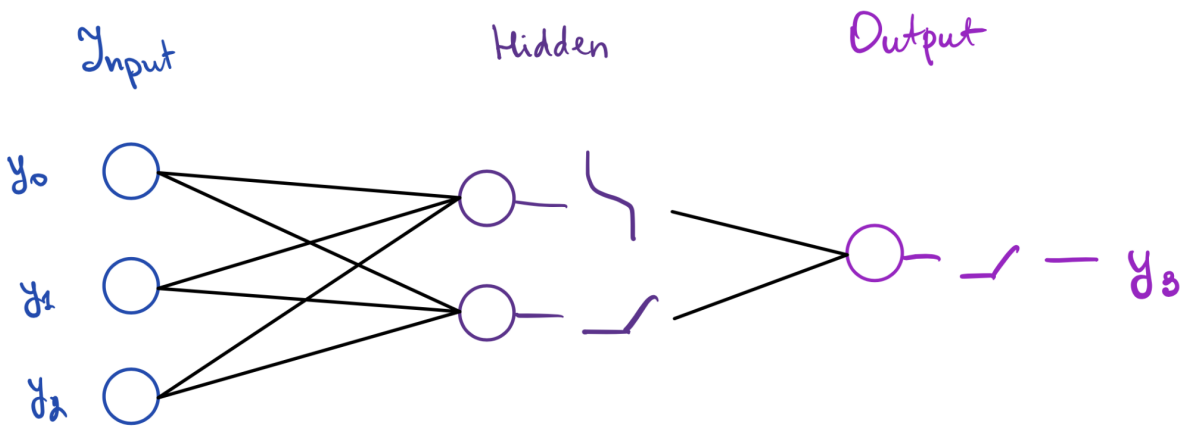

(b)

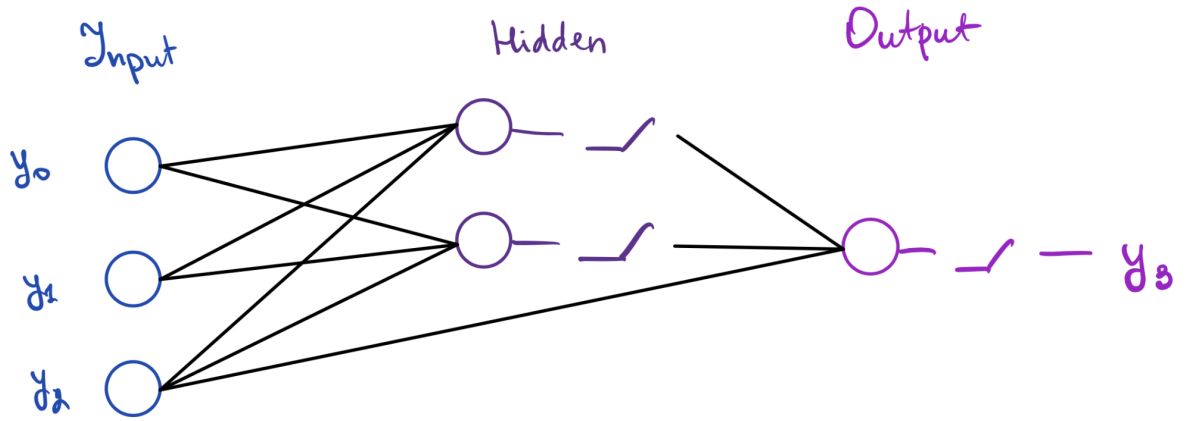

(c)

Figure 3. Feedforward neural network designs for single-step prediction. (a) Single hidden layer design with ReLU activations; (b) single hidden layer design with ReLU and Cotan activations; (c) single hidden layer with ReLU activations and direct connection from one of the input neurons to output.

All three models demonstrate a similar level of performance, as shown in Table 1, with the second model slightly outperforming the other two. Given that all the numerical data that we get from the simulator is normalized between 0 and 1, we can interpret this RMSE value as an average percent error (relative to the scene size) in predicting a single coordinate value. The network design with ReLU and cotangent activation functions seems like the best choice out of these three models.

Model	RMSE
Dense with ReLU activations	0.01827
Dense with ReLU and Cotan activations	0.01155
Dense with a direct connection from input to output	0.01819

Table 1. Comparison of root mean square errors of each of the FNN types on one-dimensional single-frame free-fall prediction.

As expected, these models make nearly perfect predictions of coordinates during the free-fall stage of the ball's movement, while having a noticeable prediction error for the frames where the bounce is observed. It can visually be noticed in Figure 4 that demonstrates the predicted "trajectory map" of the first 10 simulations from the test set by the model with ReLU and cotangent activations. Here, by "trajectory map" I mean the target coordinates within the same simulation.

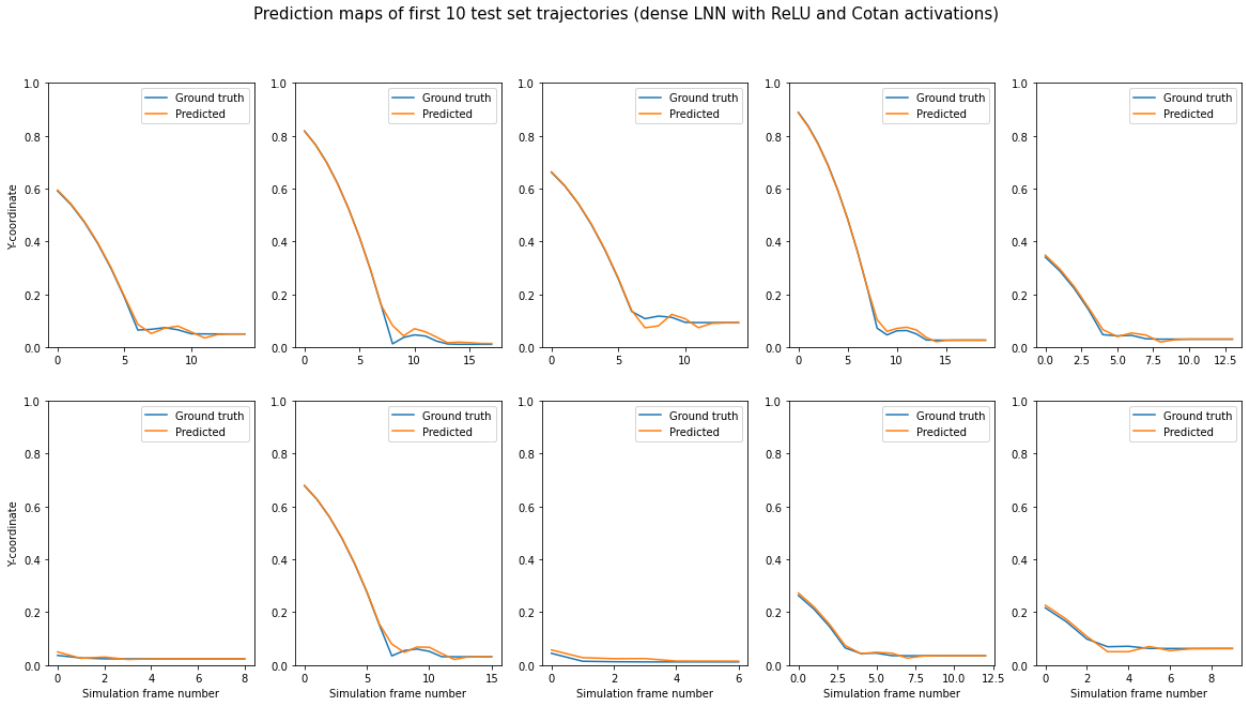

Figure 4. First 10 trajectory maps from the test set predicted by FNN with ReLU and Cotan activations.

4.1.2. Predicting the entire trajectory

While predicting the following coordinate from the three preceding is a good first research step, it doesn't have any practical value. Thus, I decided to increase the complexity of the task by bringing it closer to the goal problem - predicting the trajectory of the object from the initial state of the scene. My next step, therefore, is to train neural networks that using only the initial state will predict the entire trajectory of a free-falling ball that bounces from the ground.

I started with generating a simulated dataset, where each simulation consists of 25 frames. The y-coordinate of the ball on the first frame is separated as input to the network, while the sequence of the rest 24 coordinates is used as an output. I ended up with a dataset of 5,360 simulations, 1,072 out of which were used as a test set.

I wasn't sure if a single initial coordinate is enough information for predicting the entire trajectory. To resolve my concern, I decided to overfit my feedforward network to understand what patterns it learns from the train set, hoping that analysis of these patterns will indicate what extra data I need to include.

One of the reasons for overfitting is noise learning, which can be caused by having too large a network (Ying, 2019). I relied on this overfitting method by creating a large 5-layer linear network that takes a one-dimensional input, has four hidden layers with 256, 128, 64, and 32 neurons respectively, and outputs a vector of size 24.

After training such a model, I got an RMSE of 0.0414. The first 10 predicted trajectories with the ground truth are shown in Figure 5.

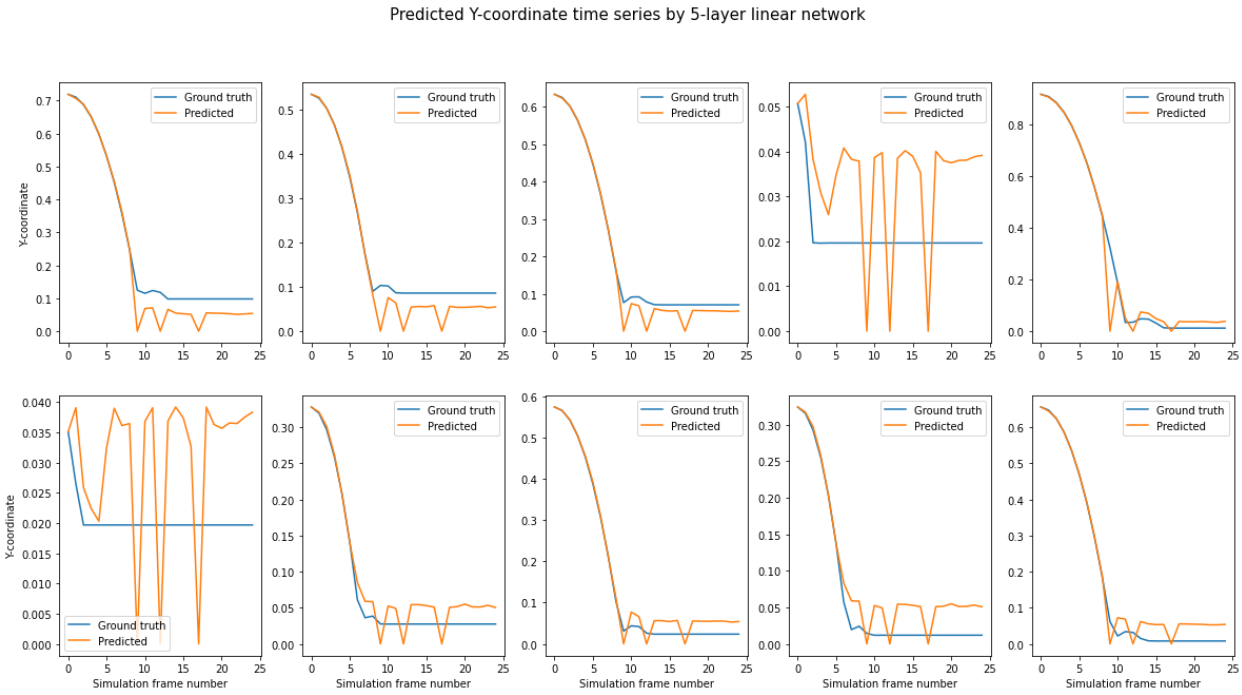

Figure 5. First 10 y-coordinate time series, ground truth, and predicted by overfitted 5-layer linear network. Plots are zoomed in to see the bounce level.

From Figure 5, which was intensionally zoomed to the scale of the whole trajectory, we can see that while the ground truth trajectory has a bounce on different levels, the model predicts it on about the same level - around 0.04-0.05 units. Seeing these results prompted me that the quantity that makes the ground truth bounce height differ is the diameter of the ball. In the absence of this information, the neural network just learns some descriptive statistics about this quantity from the training set, presumably the mean value.

To test my assumption, I modified this model to take two values as input - the initial coordinate and the ball's diameter. Testing this model on corresponding data, I received an RMSE of 0.0239 on the test set, with the first 10 predicted trajectories shown in Figure 6.

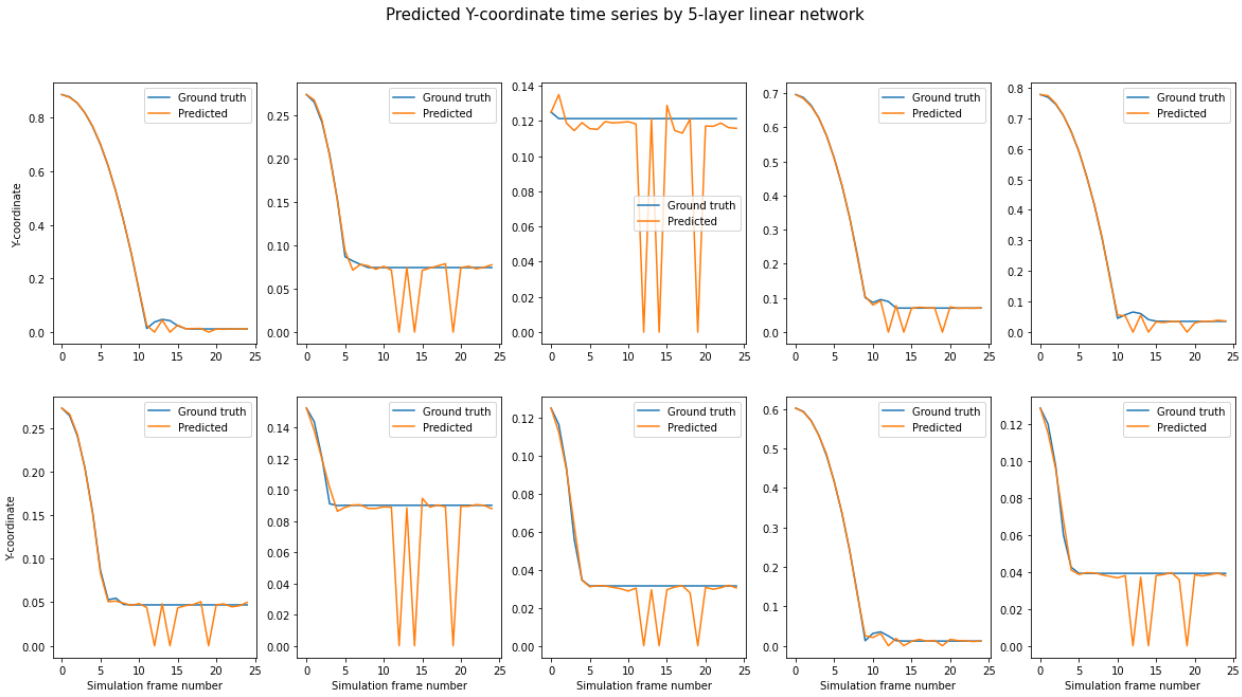

Figure 6. The first 10 trajectories from the test set, are ground truth and predicted by a 5-layer linear model that takes initial coordinate and ball diameter as input. Plots scaled to see the bounce level.

From these results, we can see that the model now predicts the bounce level correctly. The only remaining unusual pattern that we see on the plot is noise, which is not surprising given that the model is overfitted due to the large network size (Ying, 2019).

These findings conclude my exploration of feedforward neural networks. As the next steps, I will explore how recurrent neural networks will perform on the same kind of tasks.

4.2. Experiments with Recurrent Neural Networks

Recurrent Neural Networks (RNNs) are well-suited for trajectory prediction problems because they are designed to learn from sequence data (Song et. al., 2020). RNNs can make predictions based on data from previous time steps, making them ideal for trajectory prediction problems where the output of one step is used as input for the next step. RNNs are also capable of capturing long-term dependencies, which is important for predicting trajectories that span longer periods of time.

4.2.1. Traditional Recurrent Neural Networks

When it comes to predicting trajectories, there are a few neural network models that are worth considering. Vanilla RNNs are a straightforward option that is good at learning patterns over time. However, they can struggle with capturing long-term dependencies due to the vanishing gradient problem, when the gradients can become very small as they are backpropagated through time (Pascanu et. al., 2013). This can make it difficult for the network to learn long-term dependencies because the gradient signal becomes too weak to update the weights of the network effectively. GRUs are a more lightweight alternative to LSTMs and can use gating mechanisms to avoid the vanishing gradient problem. LSTMs are great at capturing long-term dependencies thanks to their memory cells and gates that selectively remember or forget information. All three models have proven to be effective for trajectory prediction tasks in areas such as robotics, autonomous driving, and video analysis. Ultimately, the choice of model depends on the specific task and the properties of the input data.

4.2.1.1. Architectures and Results

To choose an optimal RNN design, I needed to find an optimal set of hyperparameters. The hyperparameters, the optimal values of which I am aiming to find, are the number of recurrent layers, the number of hidden neurons within each layer, and the dropout rate. My goal is to optimize the test set error. Using Grid Search as an optimization method, I found that the optimal test performance is achieved with a single recurrent layer that consists of 32 hidden neurons and a zero dropout rate.

For the reason described in section 4.2.1.2. below, I had to make a slight modification of the model for testing as compared to the training. During the training stage, each of the models (Vanilla RNN, GRU, and LSTM) only consists of an input layer followed by a recurrent layer and the linear output layer. When the model is run on the test data, I added the post-processing function that bounds the outputs of the neural network between 0 and 1. The rationale behind this post-processing lies in all the data being bound between 0 and 1, so any output of the model that exceeds these bounds will not make sense. Mathematically, this post-processing function can be expressed as

$$f(x) = \max(0, \min(1, x))$$

The results of running the chosen recurrent neural networks on one-dimensional free-fall data are given in Table 2. Surprisingly, the best performance out of the three models was demonstrated by the Vanilla RNN. The first 10 predicted Y-coordinate series by each of the models are shown in Figure 7.

Model Type	**RMSE**
Vanilla RNN	0.0278
GRU	0.0304
LSTM	0.0314

Table 2. Comparison of root mean square errors of each of the RNN types on one-dimensional free-fall prediction.

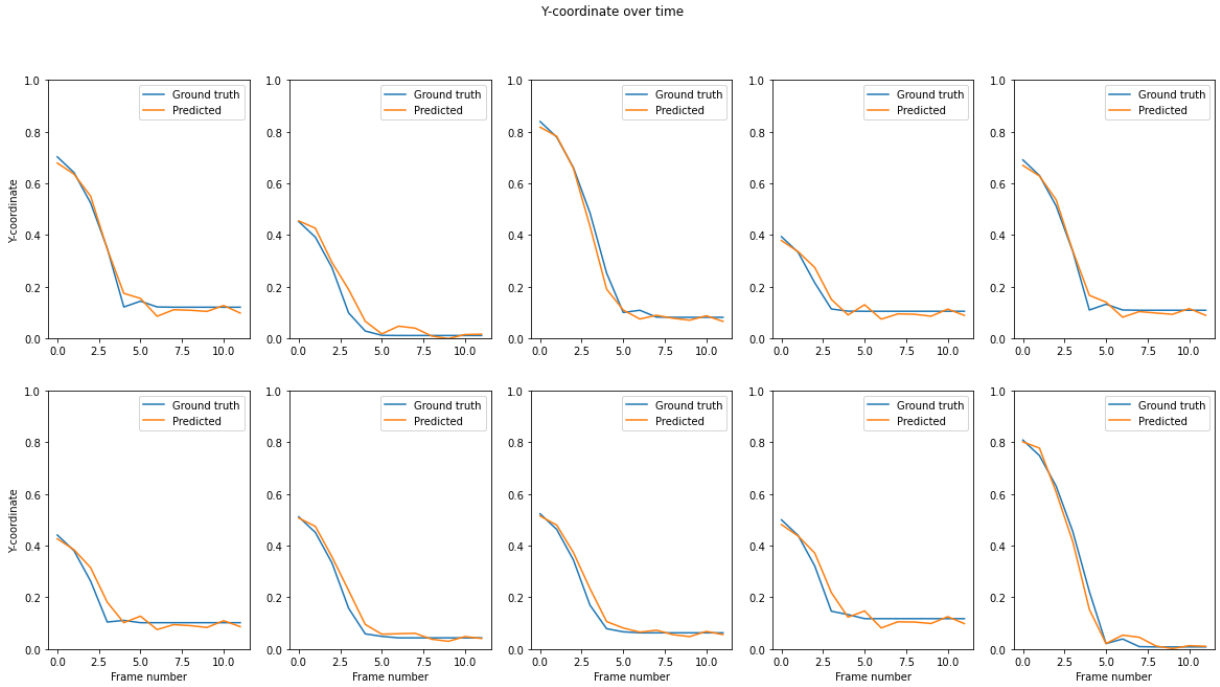

(a)

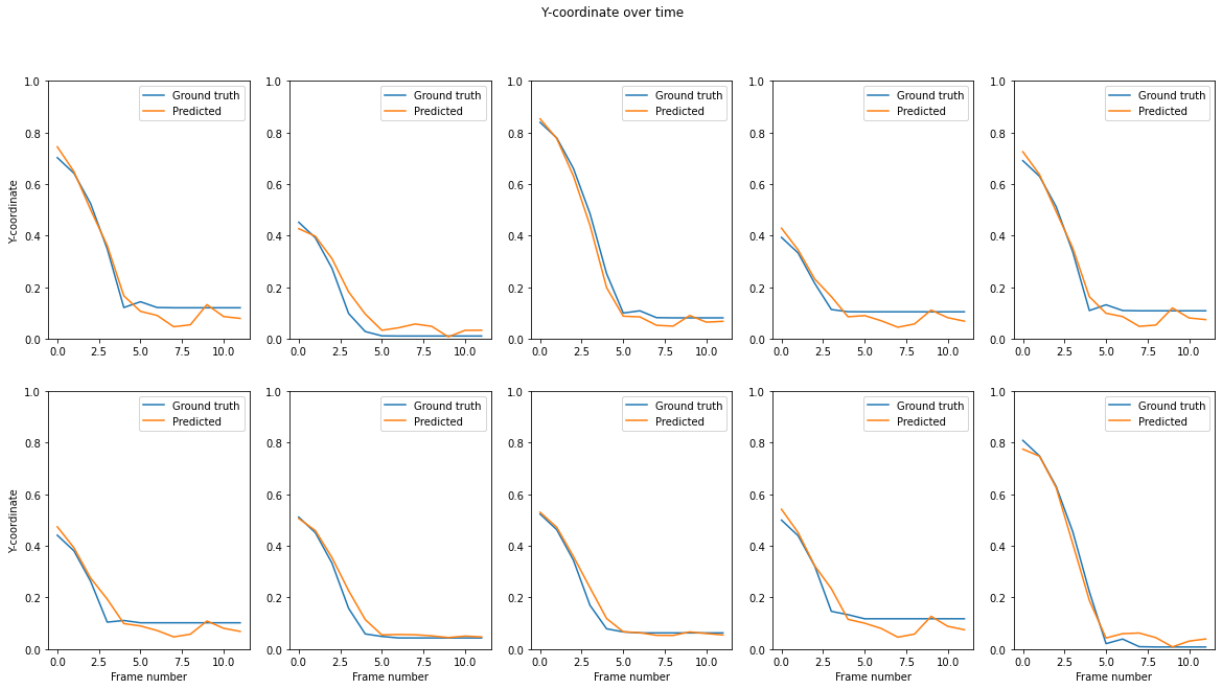

(b)

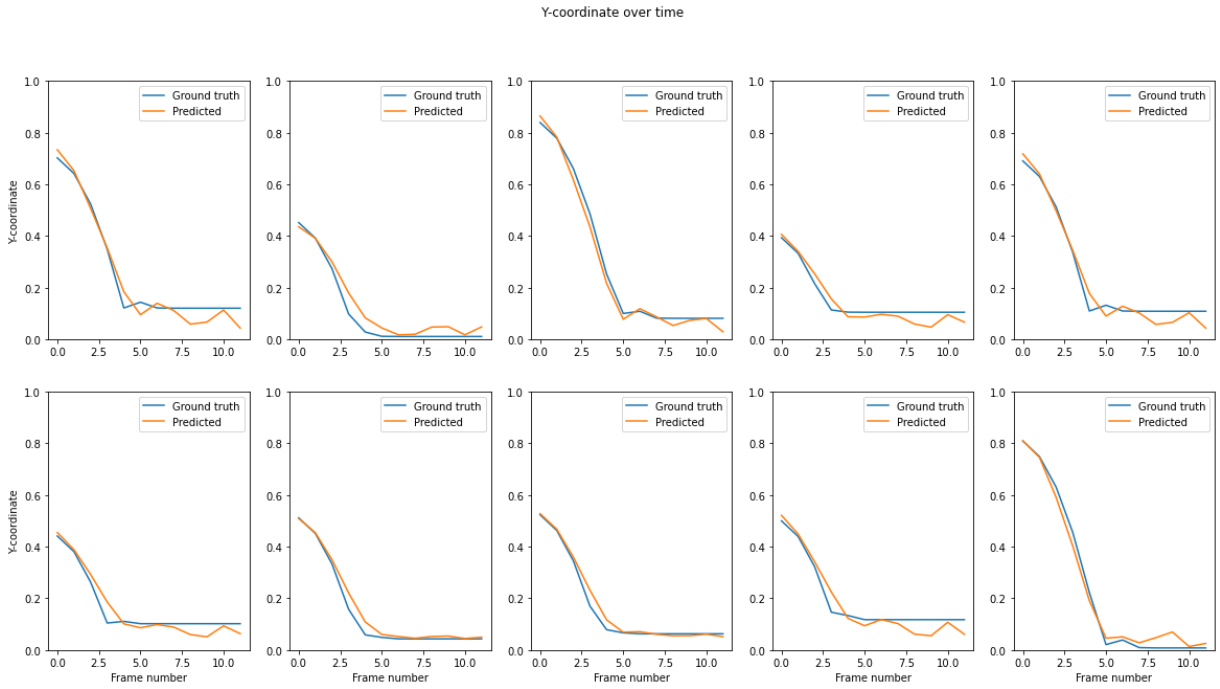

(c)

Figure 7. The first 10 predicted trajectories from the test set. (a) Vanilla RNN; (b) GRU; (c) LSTM.

4.2.1.2. Non-convergent models with ReLU layer

One of the discoveries that I had while experimenting with recurrent neural networks is that adding a ReLU activation for the final layer can noticeably decrease the model's performance. My rationale behind adding this function lies in the fact that my data is bound between 0 and 1. Adding ReLU to the final layer would prevent the model from predicting the negative values, which in theory was supposed to improve the model performance. In reality, however, the performance of each type of model decreased. Quantification of this decrease is given in Table 3, while the first 10 trajectories from the test set are shown in Figure 8. By looking at these trajectories, we can see that the models are still predicting reasonable trajectories; however, these predictions have a noise similar to that produced by overfitted feedforward neural network.

There are several reasons why this might happen. Adding a ReLU activation after the recurrent layer effectively sets the output of that layer to 0 for the negative outputs. Pascanu et. al. (2013) suggests that this causes a vanishing gradient problem, which makes it different to learn long-term dependencies. Similarly, Zaremba et. al. (2015) claims that learning long-term dependencies becomes complicated in such scenarios because the hidden states of the RNN become sparse.

Model Type	**RMSE**
Vanilla RNN with ReLU	0.1375
GRU with ReLU	0.1143
LSTM with ReLU	0.1869

Table 3. Comparison of root mean square errors of each of the RNN models with ReLU layers on one-dimensional free-fall prediction.

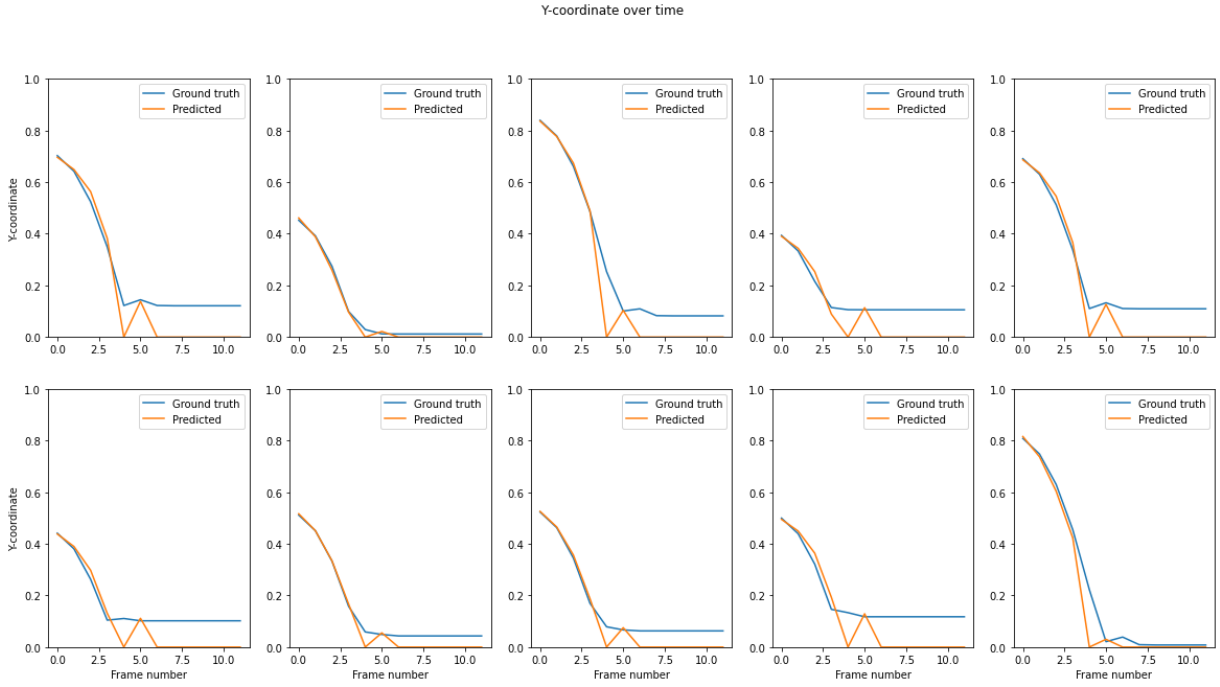
Y-coordinate over time
Ground truth
Predicted
Y-coordinate
Frame number

(a)

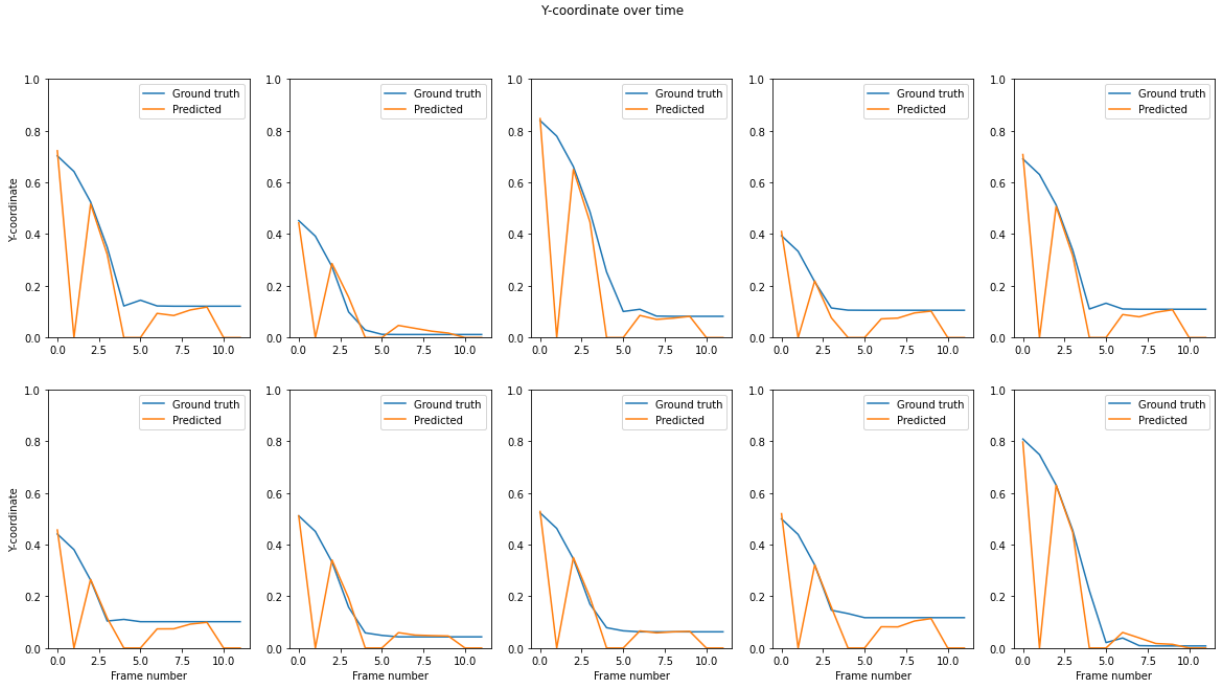
Y-coordinate over time
Ground truth
Predicted
Y-coordinate
Frame number

(b)

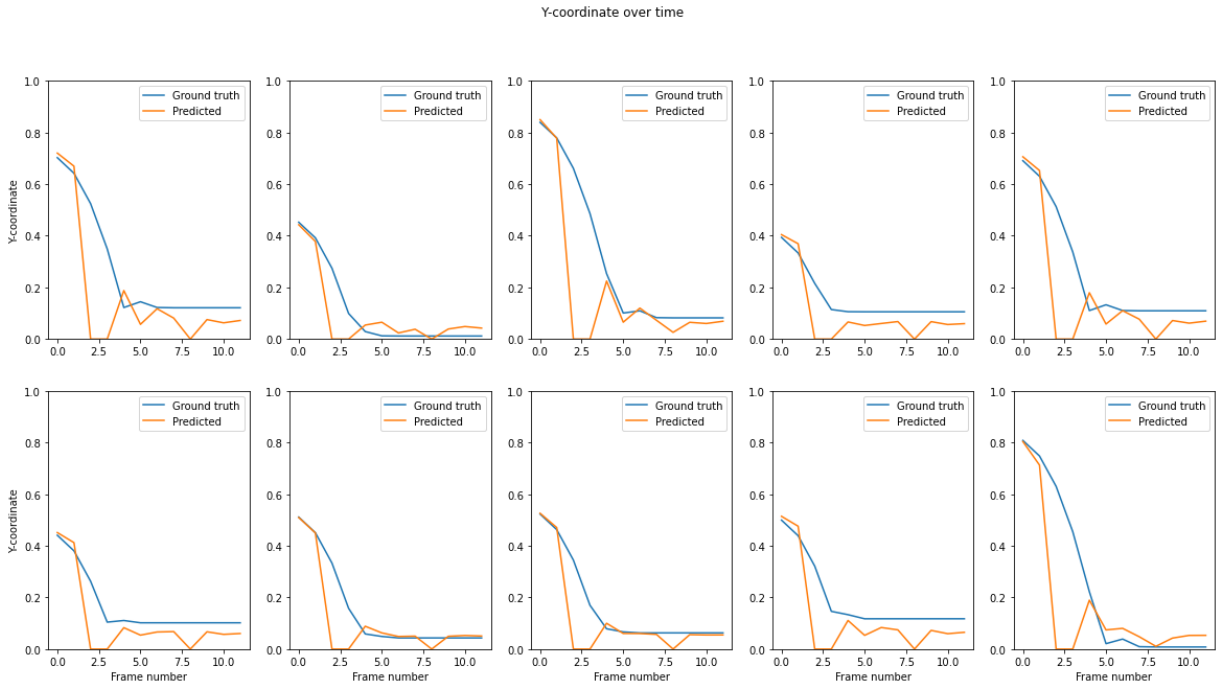

(c)

Figure 8. The first 10 predicted trajectories from the test set. (a) Vanilla RNN with ReLU; (b) GRU with ReLU; (c) LSTM with ReLU.

4.2.2. Reservoir Computing Models

While the traditional recurrent neural networks demonstrated good performance, just exploring them is not compelling research on RNNs' ability to predict trajectories. In general, if the training data is long, it becomes challenging to train RNNs due to the vanishing and exploding gradients problems (Bengio et. al., 1994). Presumably, this is what happens when I add a final ReLU layer to RNN models.

The problem of training RNNs using long data sequences is solved by the Reservoir Computing (RC) paradigm that is being actively developed over the past decade (Song et. al., 2020). Echo State Network (ESN), the most widely known RC model, "has been recognized as the most efficient network structure for training RNNs" (Malik et. al., 2016). It has also been proven to be effective for chaos prediction (Wolchover, 2018), which makes it a perfect choice for trajectory prediction problems. This is why I decided to explore various ESN architectures, including deep ESN models, for trajectory prediction tasks.

A classical Echo State Machine consists of the following components (Malik et. al., 2016):

- Input layer, neurons of which are randomly connected with the reservoir neurons.
- Reservoir - a recurrent neural network with randomly (usually not sparsely) interconnected neurons. The connectivity of neurons within the reservoir is usually quite small (around 10%). The weights of the reservoir, as well as the weights between the input and the reservoir layers, are fixed and not trainable.
- Output (readout) layer - a linear layer densely connected with the reservoir. The weights between the reservoir and the output layer are trainable and are trained in a single epoch. Typically, Ridge Regression is used as a readout layer as it is optimal for highly correlated inputs, as it happens in the reservoir, neurons of which receive responses from each other (Lukosevicius, 2012).

A schematic representation of the Echo State Network with 4-dimensional input, the reservoir of size 7, and one-dimensional output is shown in Figure 9 (Verzelli et. al., 2019).

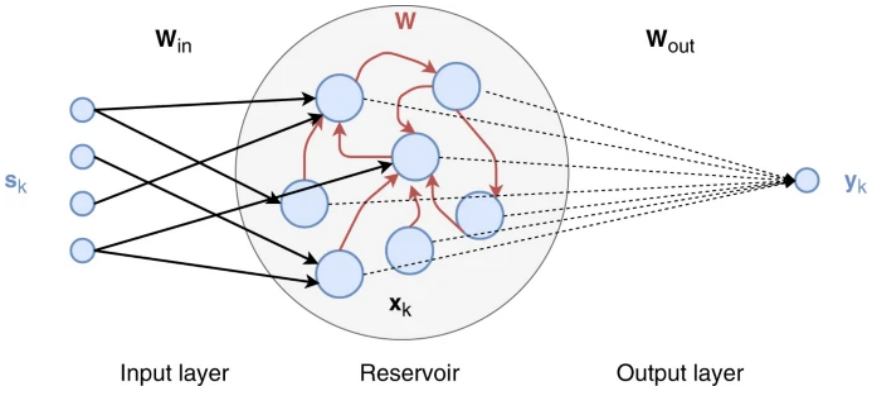

Figure 9. Echo State Network diagram with 4-dimensional input, the reservoir of size 7, and one-dimensional output. Retrieved from "Echo State Networks with Self-Normalizing Activations on the Hyper-Sphere" (2019) by Verzelli, P., Alippi, C., and Livi, L.

4.2.2.1. Architectures and Results

I started with testing out how different Echo State Network architectures will perform on predicting one-dimensional free-fall with a bounce. To implement the models, I used a Reservoirpy framework created by Trouvain et. al. (2020).

To test the ability of ESNs to predict trajectories, I implemented several different architectures. I started with a simple single reservoir Echo State Network, the number of hyperparameters of which allows to run Grid Search to find their optimal set. I found out that the optimal hyperparameters of ESN with Ridge Regression Readout for free-fall prediction are:

- Reservoir size of 70 neurons;
- Leaking rate of 0.7;
- Spectral radius of 0.95;
- Ridge coefficient of 0.01.

A number of papers, among which are papers by Malik et. al. (2016) and Song et. al. (2020), suggest that Deep Echo State Networks show better performance when compared to classical ESNs. Conducting a Grid Search for deep architectures would take an exponentially longer time compared to the classical ESN due to the increased number of parameters. Specifically, even adding a single extra reservoir adds 3 more hyperparameters (reservoir size, leaking rate, and spectral radius of the new reservoir) that, ideally, need to be optimized in addition to those of the first reservoir. While I don't have enough computational resources to run a Grid Search for hyperparameter optimization in Deep ESNs, I decided to take the optimal set that I found for the simple ESN and use it while creating Deep ESN models. The deep models that I tried for the free-fall prediction are

- Sequential ESN, inspired by Multilayered ESN presented by Malik et. al. (2016). I modified the model presented in this paper by adding a readout layer between each pair of reservoirs. The rationale behind it is that stacking several reservoirs without the readout layer is not different in principle from having a single reservoir with a larger size and modified connectivity;
- Parallel ESN, suggested by Song et. al. (2020);
- Grouped ESN, suggested by Song et. al. (2020).

All four types of ESN (classical plus three deep architectures) are schematically shown in Figure 10.

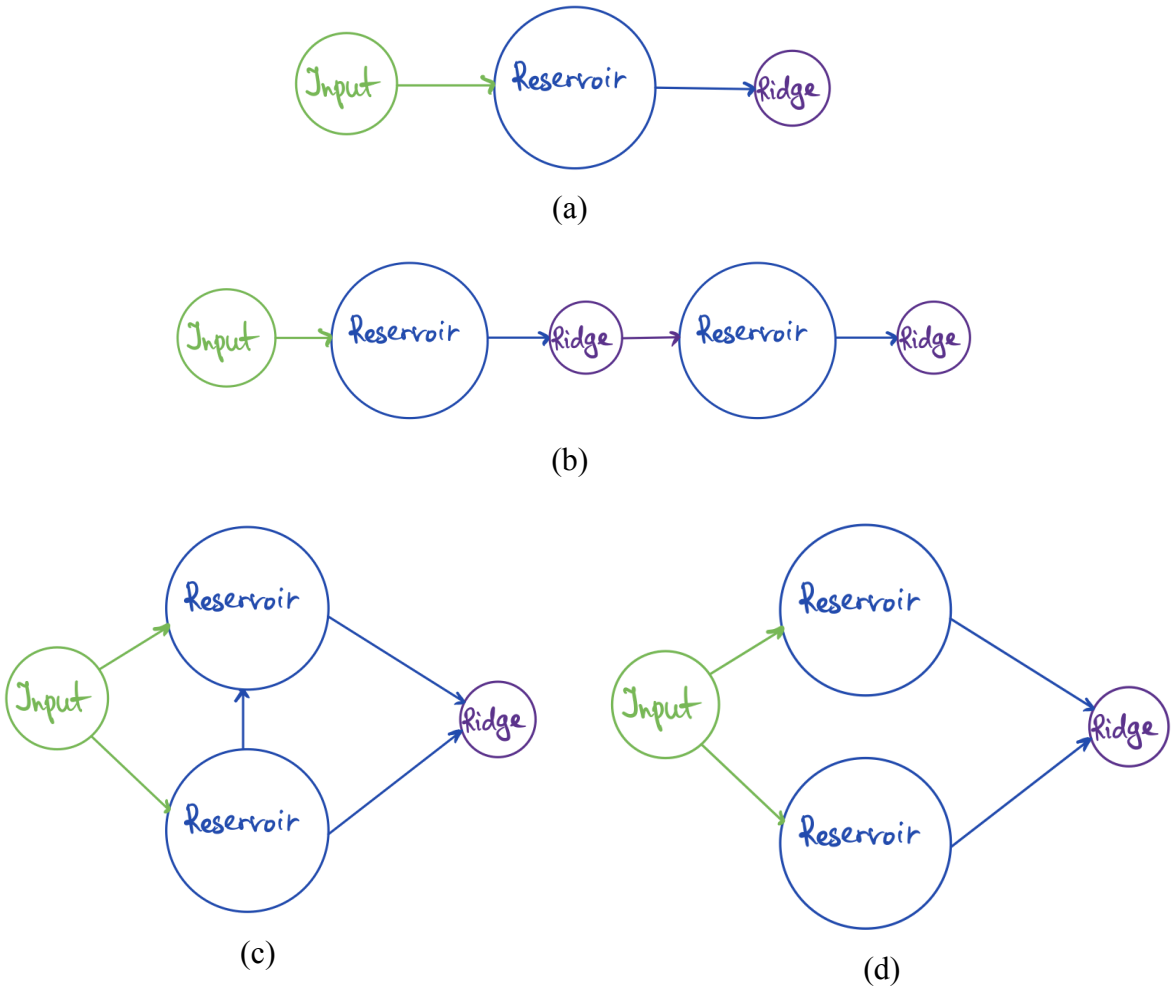

Figure 10. Implemented Echo State Network Architectures. (a) Classical ESN; (b) Sequential ESN; (c) Parallel ESN; (d) Grouped ESN.

It is easy to note that if any of the deep architectures will consist of a single reservoir, it will correspond to a simple ESN. To test the performance of these models, I trained a simple ESN as well as all the deep models with a number of reservoirs between 2 and 10. The performance of each of all of these models on the test set is shown in Figure 11, where the first point in every plot corresponds to the performance of a simple ESN.

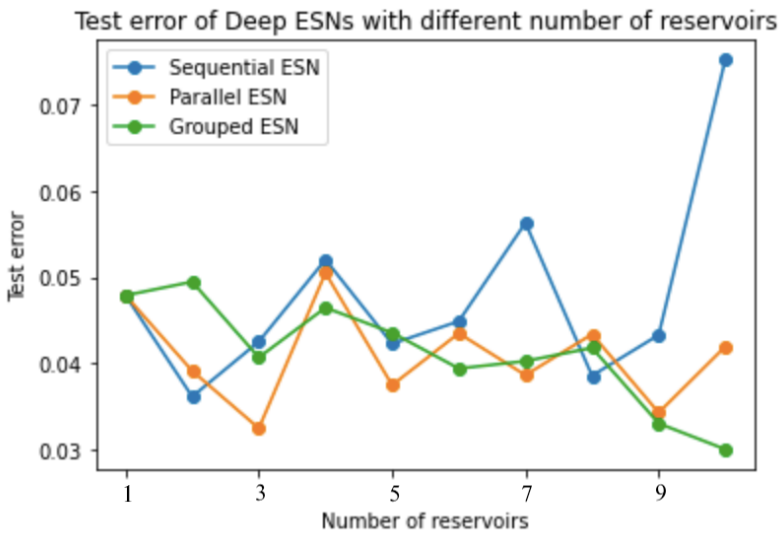

Figure 11. Performance of the Echo State Networks on the test set as a function of the number of reservoirs.

We can see that, perhaps with the exception of Grouped ESN, increasing the number of reservoirs doesn't improve the test set performance. Moreover, we can see that all of these models perform slightly worse when compared to the traditional recurrent neural networks. The first 10 test set trajectories for simple ESN and each of the deep ESN with two reservoirs are shown in Figure 12.

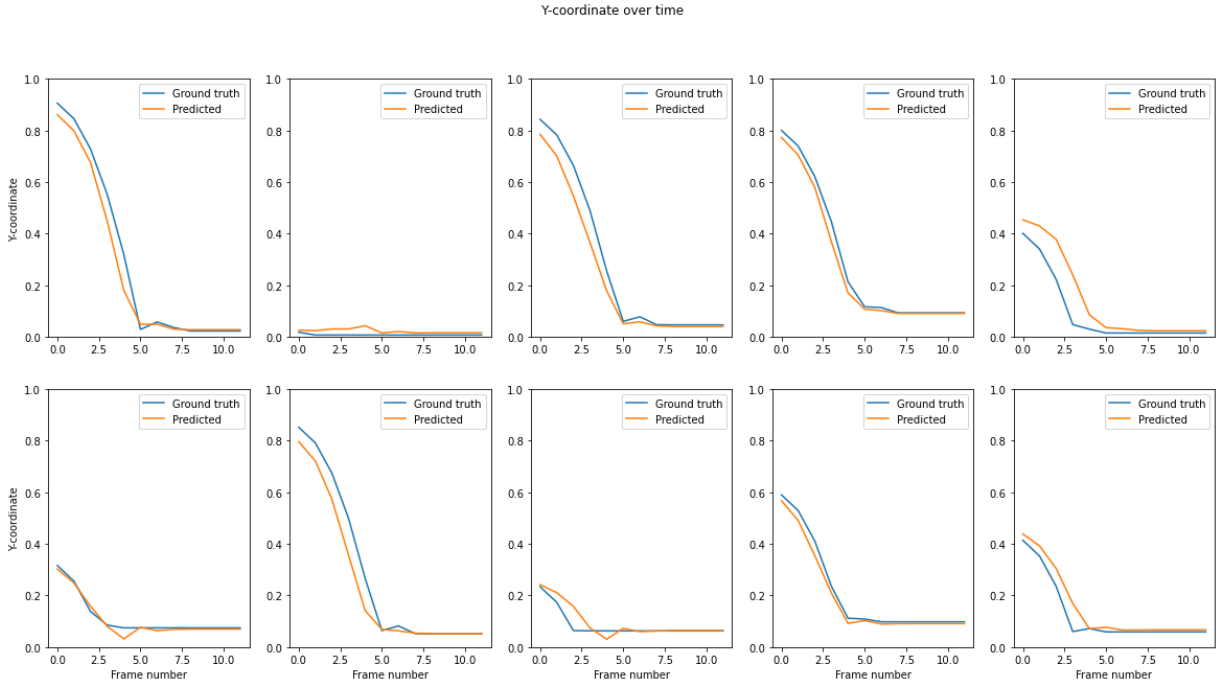
Y-coordinate over time
Ground truth
Predicted
Y-coordinate
Frame number

(a)

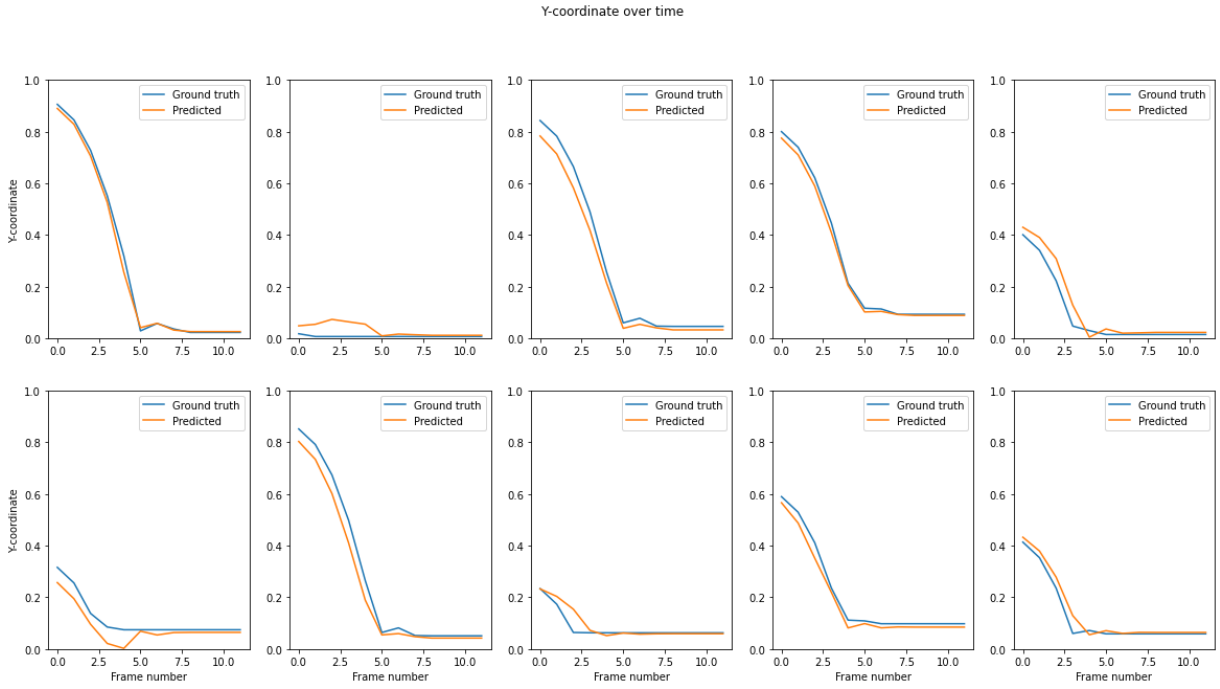
Y-coordinate over time
Ground truth
Predicted
Y-coordinate
Frame number

(b)

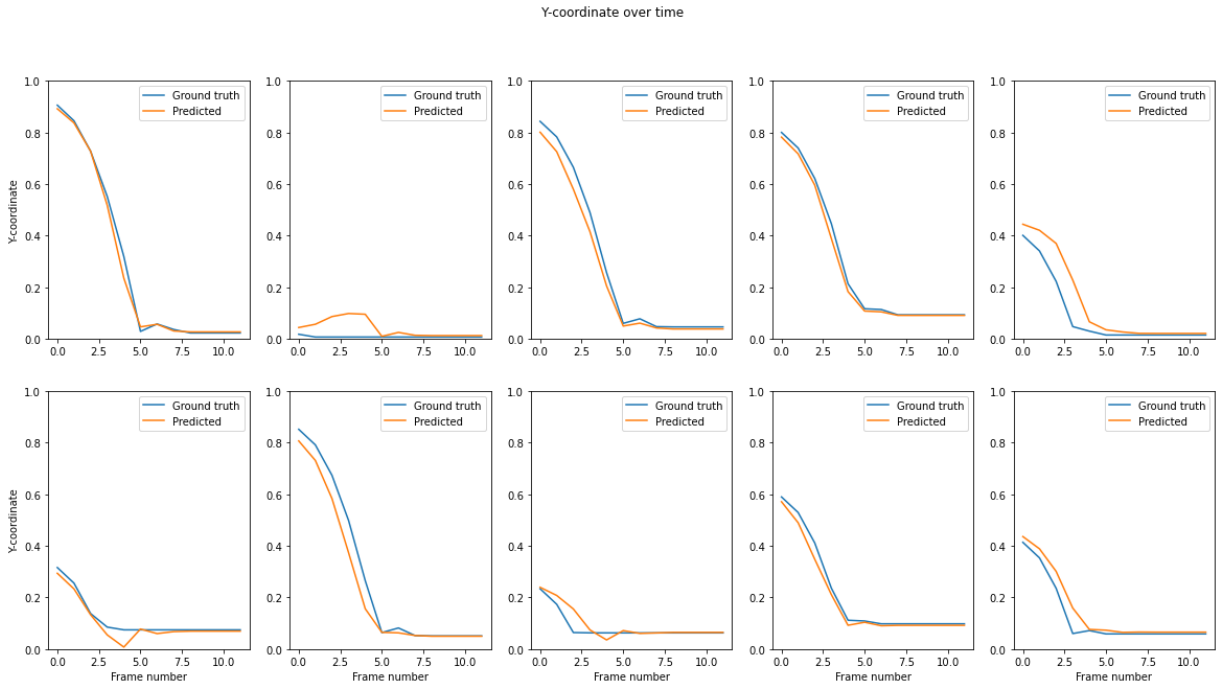

(c)

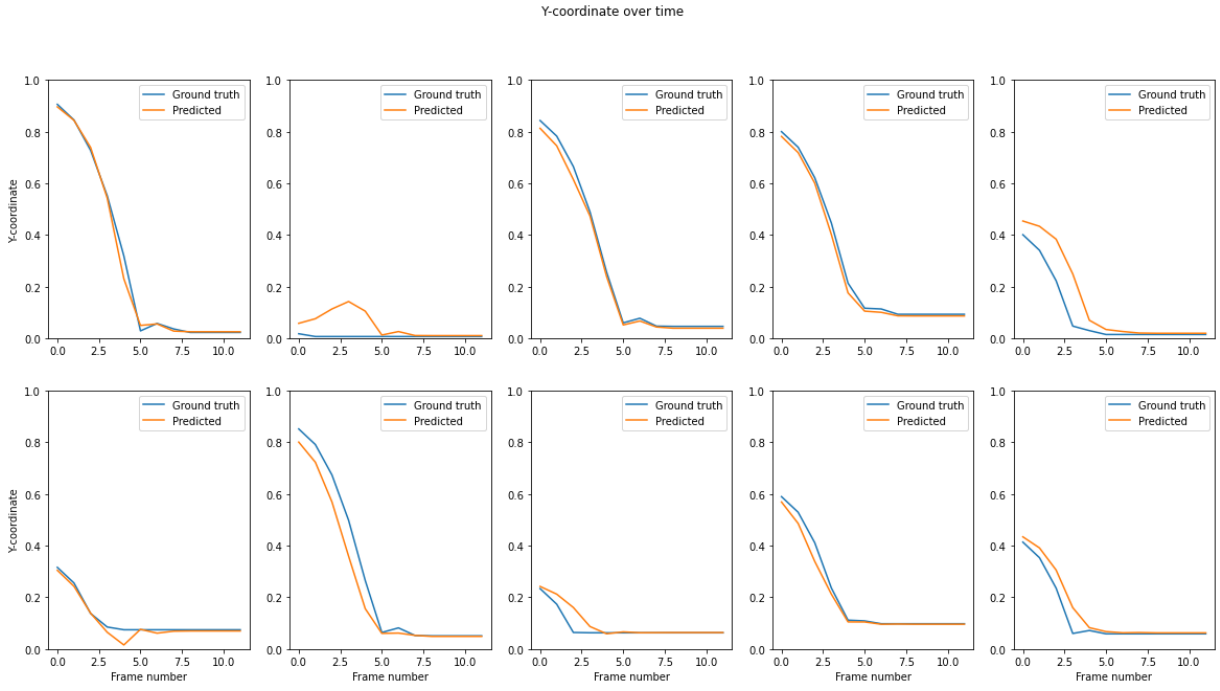

(d)

Figure 12. First 10 test set predicted trajectories by Echo State Networks. (a) Simple ESN; (b) Sequential ESN; (c) Parallel ESN; (d) Grouped ESN.

4.2.2.2. ReLU layer experiment

After noticing that adding the ReLU layer prevents the training of traditional RNNs to converge properly, I decided to check if adding this layer also affects the performance of Echo State Networks. To do it, I decided to run an experiment on two ESN models, the only difference between which is the presence or absence of the final ReLU layer. My null hypothesis is that the mean test errors will be the same for both models, with an alternative hypothesis that the mean error will be less for the model *without* the final ReLU layer. I decided to make a decision on whether to reject the null hypothesis based on the t-test with a 0.05 significance level.

To perform the test, I generated two relatively small datasets (1,110 free-fall simulations). Then, I made 80 random train-test splits with a test fraction of 0.2 (222 simulations), and for each of these splits, I trained both models and saved the resulting test loss. A sample size of 80 for each model is chosen for Central Limit Theorem to hold properly. Once training and calculating test loss is complete for each split and each model, I run the difference of means test. I got a p-value of 0.22 on the one-tailed test, which is insignificant on the chosen significance level. This means that the test failed to reject the null hypothesis, or, in other words, the presence of the final ReLU layer doesn't make the performance of the model worse. The histogram of the test losses is given in Figure 13.

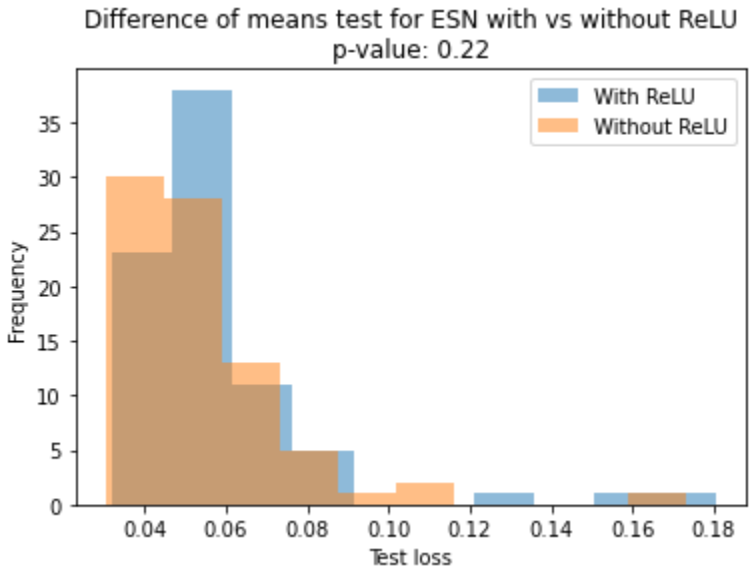

Figure 13. Histogram of test losses for ESNs with and without final ReLU layer.

4.2.3. Generalizing free-fall scenarios

Now that the one-dimensional free-fall is explored, there are a few more intermediate steps that need to be done to come closer to the trajectory prediction tasks in scenarios with collisions.

4.2.3.1. Free-fall in two dimensions

Up to this point, I was using a single Y-coordinate, knowing that X-coordinate stays constant during the free-fall. Now I want to test if my models will be able to infer that this coordinate is constant.

For this purpose, I generated a new dataset that includes X-coordinate in the output. I simulated 52,810 scenarios, 10,562 out of which were used as a test set.

Running a Grid Search for two-dimensional free-fall prediction resulted in the same optimal set of hyperparameters for Echo State Network models as for the one-dimensional scenarios. For traditional Recurrent Neural Networks, while a single recurrent layer was still found to be optimal, the number of hidden layers needs to be increased to 64.

While it is incorrect to compare the errors between one and two-dimensional free-fall predictions *to make any inference*, I was expecting the error to rise due to the increased output dimension to have an approximately matching error per predicted value. However, an interesting finding is that for all types of models that I tried, the test error noticeably decreased, although the number of parameters that need to be predicted increased two times.

The test set error for each of the models is given in Table 4. The first 10 predicted y-coordinate sequences and full trajectories from the test set are shown in Figure 14.

Model	**RMSE**
Vanilla RNN	0.0182
GRU	0.0160
LSTM	0.0164
ESN	0.0320

Sequential ESN	0.0413
Parallel ESN	0.0314
Grouped ESN	0.0314

Table 4. Root mean square error of each model on the test set for two-dimensional free-fall prediction.

We can see that the Reservoir Computing models perform noticeably worse compared to the traditional RNNs. From Figure 14, however, we can notice a significant difference in the predicted trajectories: while traditional RNNs do a good job predicting the free-fall trajectories very closely, we can still see oscillations in predicted values for both coordinates. Meanwhile, ESNs do a worse job resembling the trajectories closely; however, they perfectly learn that free-fall is happening along a straight line.

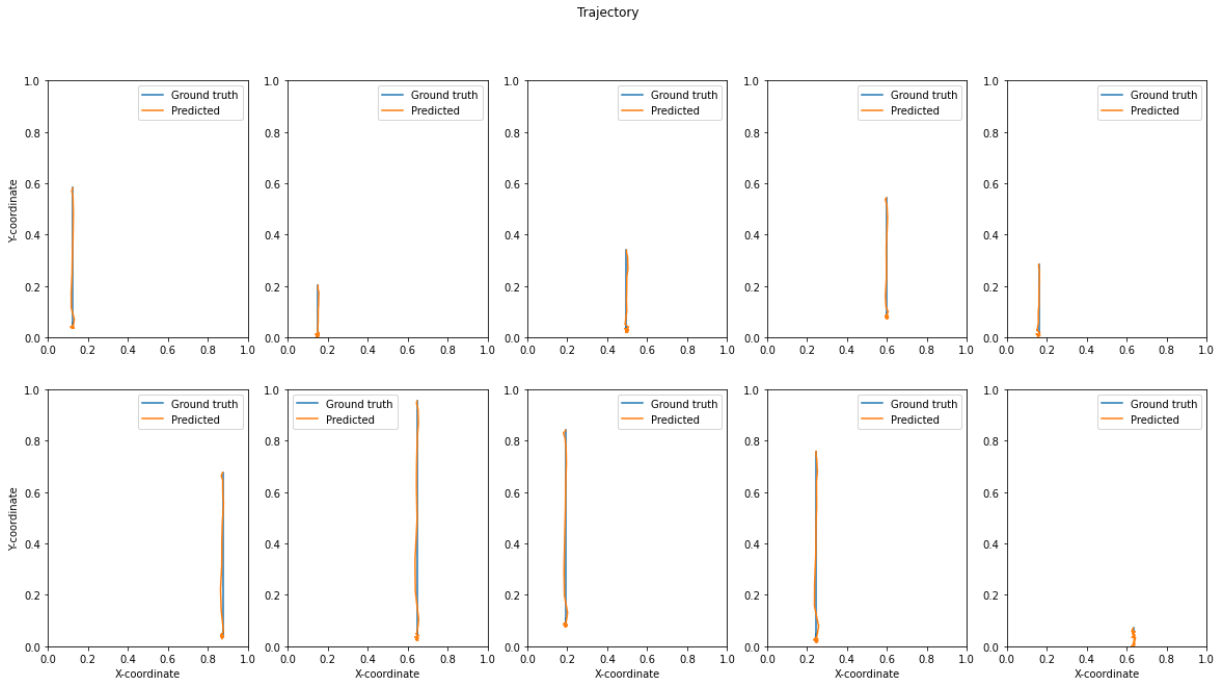

(a)

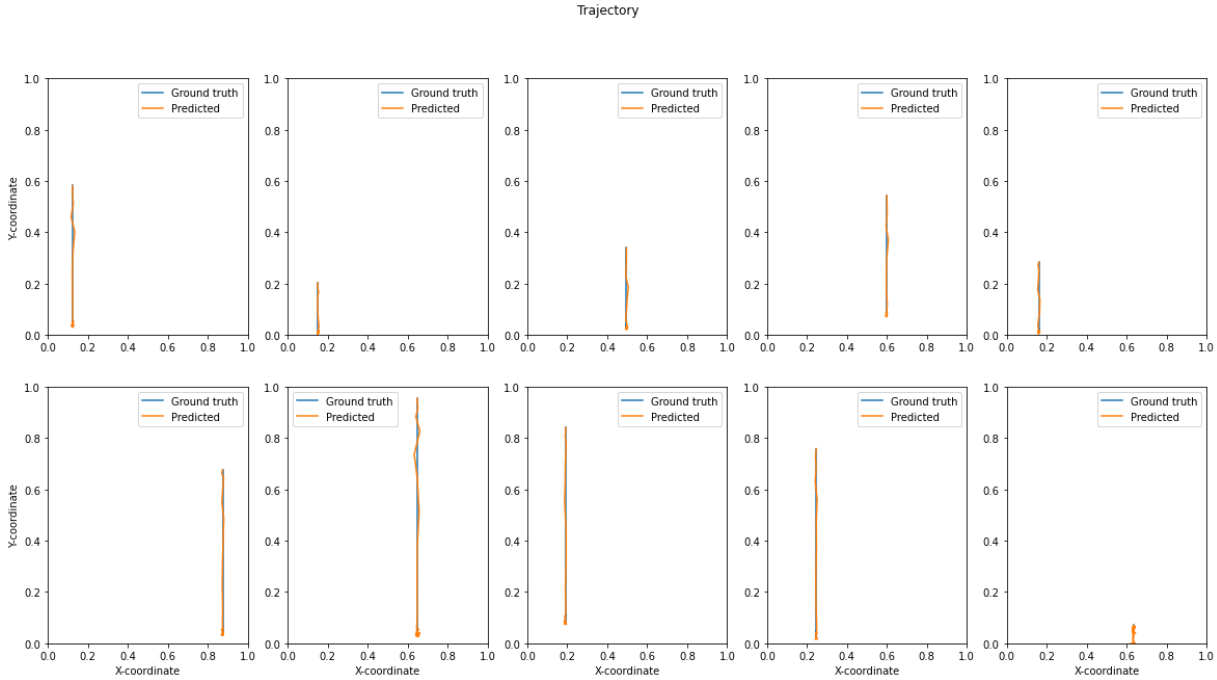
Trajectory
Ground truth
Predicted
Y-coordinate
X-coordinate

(b)

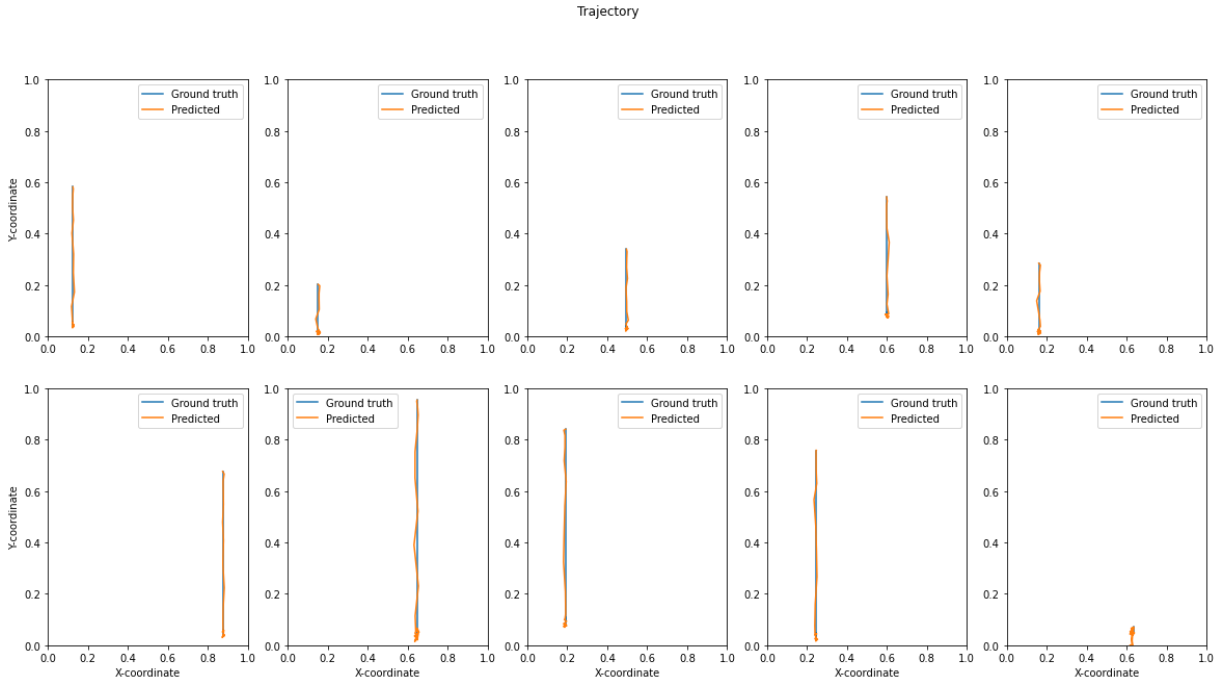
Trajectory
Ground truth
Predicted
Y-coordinate
X-coordinate

(c)

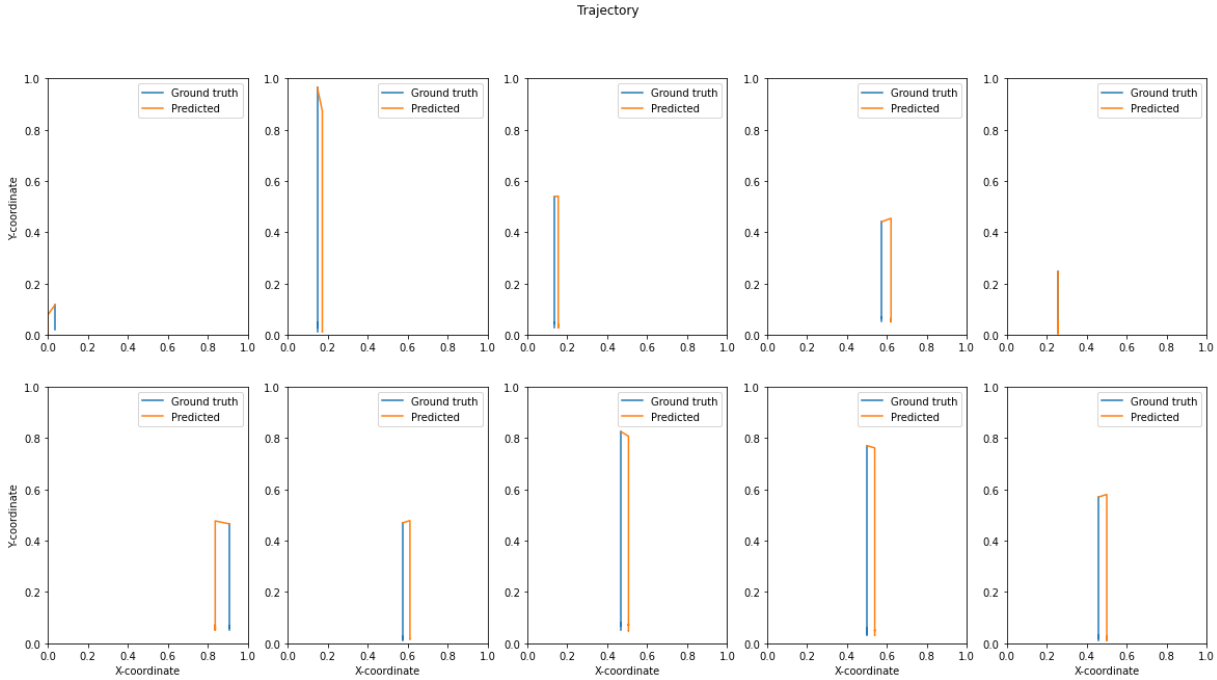
Trajectory
Ground truth
Predicted
Y-coordinate
X-coordinate

(d)

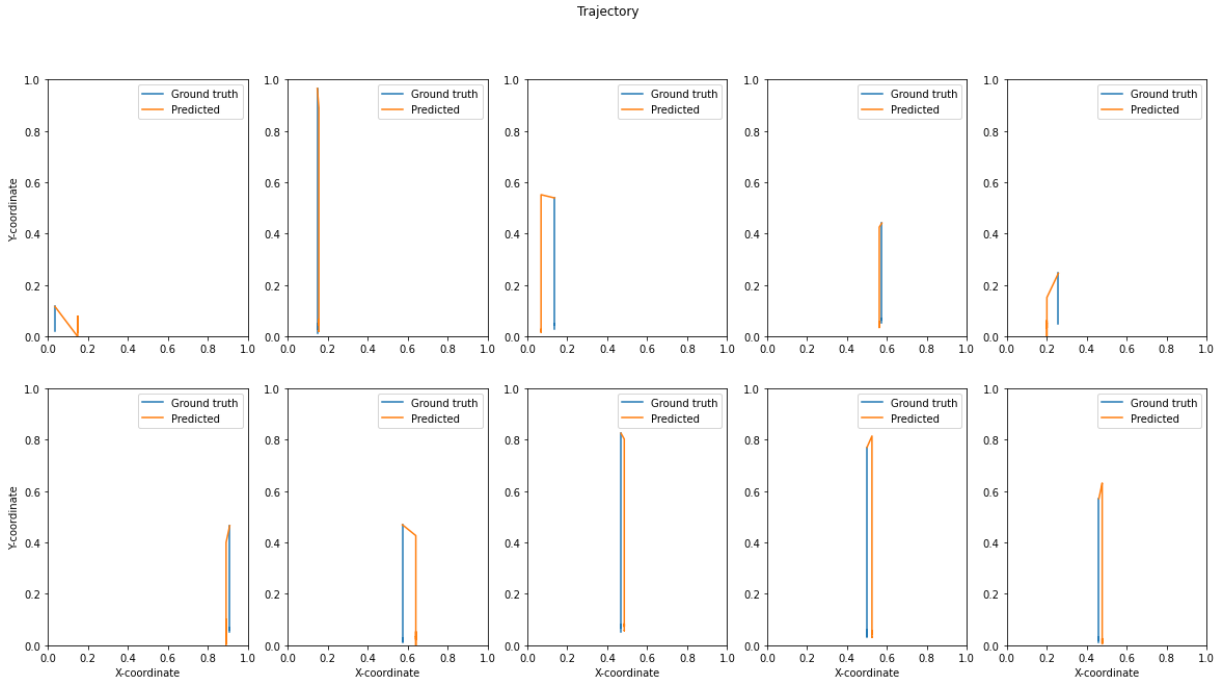
Trajectory
Ground truth
Predicted
Y-coordinate
X-coordinate

(e)

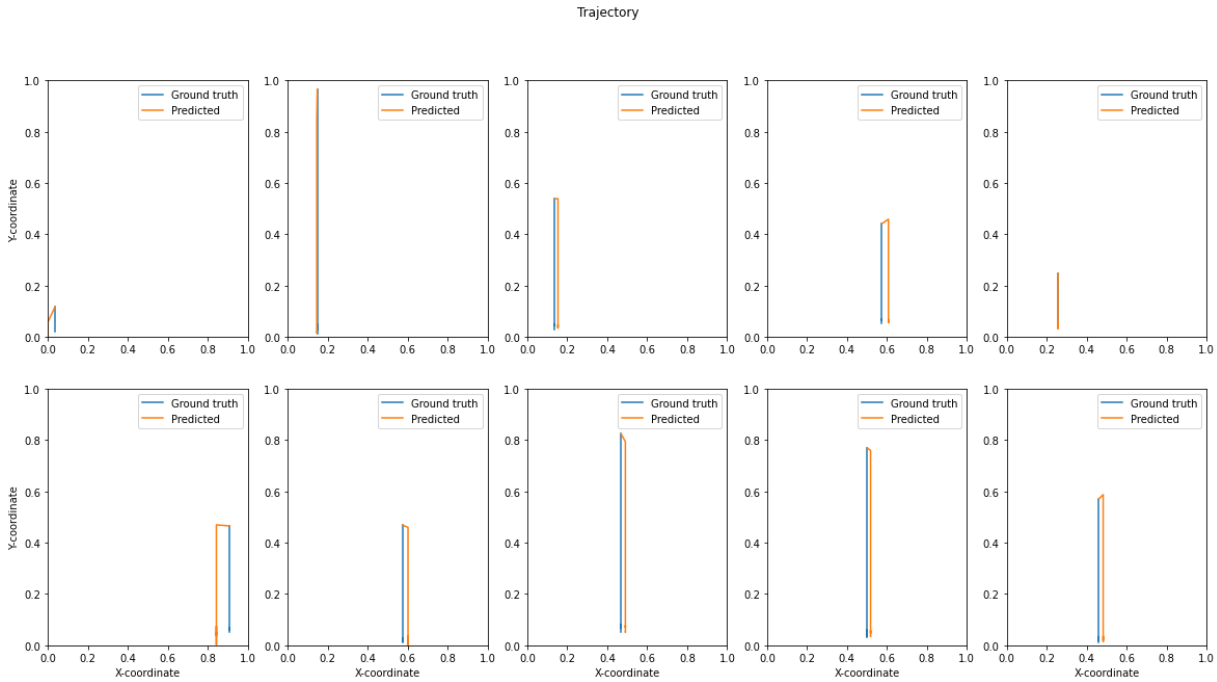

(f)

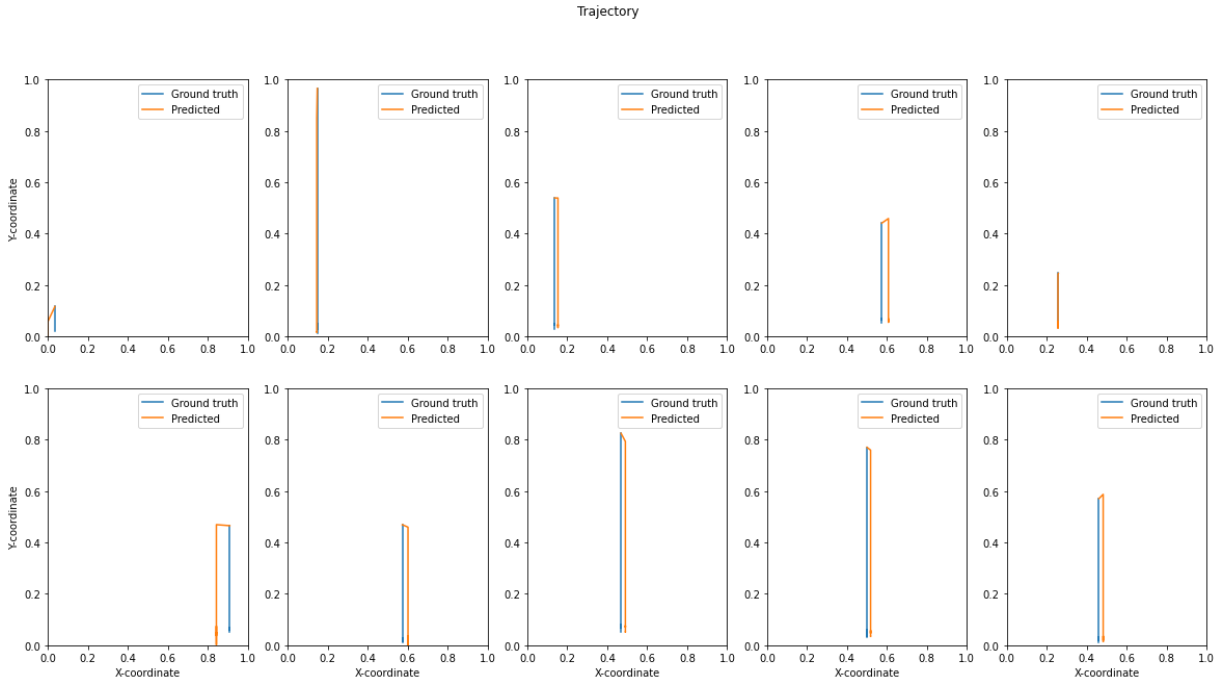

(g)

Figure 14. Predicted two-dimensional free-fall trajectories by each of the models. (a) Vanilla RNN; (b) GRU; (c) LSTM; (d) ESN; (e) Sequential ESN; (f) Parallel ESN; (g) Grouped ESN.

4.2.3.2. Scenarios with multiple balls

The last layer of complexity that I can add to predicting the free-fall trajectory of the ball is adding information about other balls on the scene to the input.

Table 5 shows the free-fall prediction RMSE value of each of the models on the test set. As we can see, adding extra information to the input did not affect the performance of the traditional models, while the performance of Reservoir Computing models actually improved. My hypothesis is that the extra input serves as the extra variable for regularization in Ridge Regression, which positively affects the model performance.

Model	**RMSE**
Vanilla RNN	0.0194
GRU	0.0165
LSTM	0.0158
ESN	0.0251
Sequential ESN	0.0374
Parallel ESN	0.0257
Grouped ESN	0.0257

Table 5. RMSE of predictions on the test set for free-fall scenarios with multiple balls.

4.3. Intermediate Conclusion

In this section, I investigated the performance of various Recurrent Neural Network architectures in predicting the trajectory of a ball undergoing free fall and bouncing off the ground. A thorough comparison between traditional RNNs and Reservoir Computing models revealed that traditional RNNs outperform their counterparts in minimizing prediction errors. However, a closer examination of the visualization of the models' predictions suggested that RC models may have a better grasp of the underlying physics of free-fall motion.

A prime example of this is demonstrated in the two-dimensional free-fall prediction task. While traditional RNNs achieve lower error rates, they struggle to capture the fact that free-fall occurs

strictly along a straight line. In contrast, RC models successfully learn this pattern but fail to accurately determine the specific x-coordinate along which the free-fall occurs.

In conclusion, this section highlights the strengths and weaknesses of both traditional RNNs and Reservoir Computing models in the context of trajectory prediction for free-falling objects. While traditional RNNs excel at minimizing prediction errors, RC models demonstrate a better understanding of the underlying motion patterns, despite their shortcomings in accurately predicting specific trajectories. This insight may guide future research on developing hybrid or improved models that can leverage the strengths of both architectures for more accurate and physically plausible trajectory predictions.

Section 5. Movement with collisions

In this section, I will address the challenges associated with the increased complexity of scenarios involving three balls falling and colliding with each other. The larger datasets required for these scenarios lead to longer training times, making hyperparameter optimization more difficult. To tackle these challenges, I will discuss two aspects of data engineering that need to be reconsidered: limiting the number of free-fall scenarios and optimizing the use of data for hyperparameter optimization and model training.

5.1. Optimizing data engineering

While my focus now shifts from free-fall scenarios to those involving collisions, randomly sampling actions will still include a significant number of scenarios where the target ball is still in free fall. To ensure that my dataset adequately represents the more complex collision scenarios, I will need to limit the fraction of free-fall scenarios in the dataset. I will discuss the method that I used to limit the number of free-fall scenarios in section 5.1.1.

As the dataset size increases and training times become longer, it is crucial to use the available data efficiently for hyperparameter optimization and model training. In section 5.1.2 I will discuss how I changed my approach to hyperparameter optimization to deal with a large dataset.

5.1.1. Limiting the fraction of free-fall scenarios

In the current approach to generating datasets, as discussed in section 3.2, random actions are sampled, resulting in a high fraction of free-fall scenarios even when not constrained to them. This can lead to biased model predictions towards free-fall, and thus, the number of free-fall scenarios in the dataset must be constrained. Since Phyre doesn't provide an API for implementing such constraints, I will propose an alternative approach.

Let’s define:

- t as the total number of valid simulations;
- f as the number of free-fall scenarios among t;
- ϵ as the desired fraction of free-fall scenarios;

- r as the number of free-fall simulations that need to be removed from the pool.

We can detect the free-fall simulations as those where the x-coordinate of the red ball stays constant.

To limit the fraction of the free-fall simulations to ϵ, I need to remove r free-fall simulations such that the following equation holds:

$$\frac{f-r}{t-r} = \epsilon$$

From this equation I can express the number r of the simulations that need to be removed.

$$r = \frac{f-\epsilon t}{1+\epsilon}$$

Thus, the strategy is to simulate some number of scenarios, labeling the free-fall simulations in some special way. Once the whole dataset is generated, randomly sample r free-fall simulations, according to the chosen fraction ϵ, and remove them from the dataset. This will result in a dataset with a more balanced representation of free-fall and collision scenarios, allowing the model to better generalize to the task of predicting trajectories in scenarios with collisions.

5.1.2. Changing the data usage for training vs. hyperparameter optimization

In scenarios where the ball's movement is not constrained in 1 dimension and interacts with other balls, the complexity increases, necessitating more data for training machine learning models to predict such movements. However, more data leads to longer training times and exponentially longer Grid Search computations for hyperparameter tuning.

To address this issue, I will generate two separate datasets for training and hyperparameter tuning, with their size being the only difference. For hyperparameter tuning, I will create a relatively small dataset. It is acknowledged that the smaller dataset might result in inadequate training of the models, leading to a suboptimal final performance. However, the assumption is that despite each model being undertrained, their relative performance when trained on the smaller dataset should be preserved compared to the larger dataset.

For hyperparameter tuning, I created two datasets (for predicting single-ball trajectory and evolution of the entire scene, as discussed in sections 5.2 and 5.3, respectively) containing 18,186 simulations each, 3,637 of which were used as hold-out sets. Once the optimal set of hyperparameters is found for each model using this dataset, I can use them to train the models using bigger datasets. The bigger datasets contain 274,056 simulations each, 54,811 of which were used for testing.

5.2. Predicting single ball trajectory

I started with running the Grid-Search for each of the traditional model types. The search space that I had was the following:

- Number of hidden neurons: 64, 96, 128, 192, 258;
- Number of recurrent layers: 1, 2, 3;
- Dropout rate (for the number of layers greater than 1): 0, 0.1.

For all three models, the optimal set of hyperparameters found with Grid Search is 96 neurons, 1 recurrent layer, and 0 dropout rate. The test set RMSE of traditional RNN models is shown in Table 6, which indicates a threefold decrease in performance compared to predicting solely free-fall with similar input.

Model	**RMSE**
Vanilla RNN	0.0467
GRU	0.0487
LSTM	0.0426

Table 6. RMSE of traditional models on predicting trajectories with collisions from the test set.

Figures 15-17 illustrate the predicted trajectories by each traditional model, along with the predicted x-coordinate and y-coordinate time series. Each coordinate prediction exhibits significant noise, and this noise persists even when increasing the dataset size threefold (from 91,256 simulations that I used originally to 274,056 simulations that were used to produce the reported results). Among the three models, LSTM produces the least noisy predictions, though

they are still not highly accurate. While the models correctly predict the object's downward motion, they often fail to accurately infer collisions and post-collision movements.

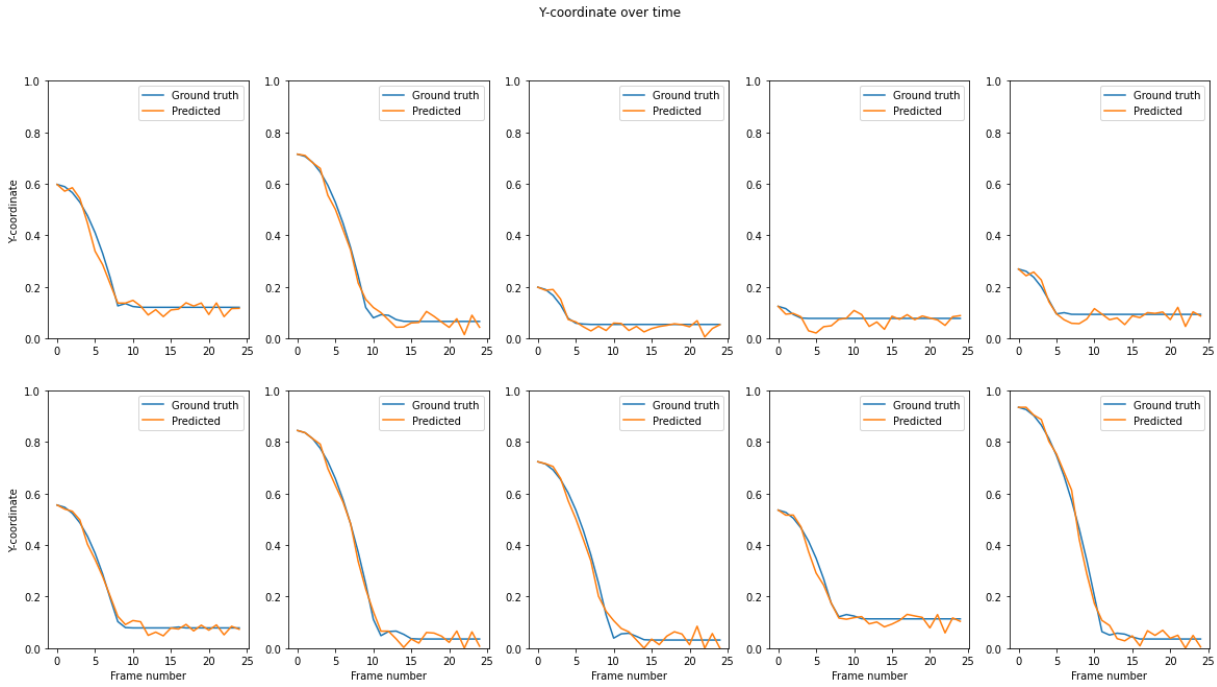

(a)

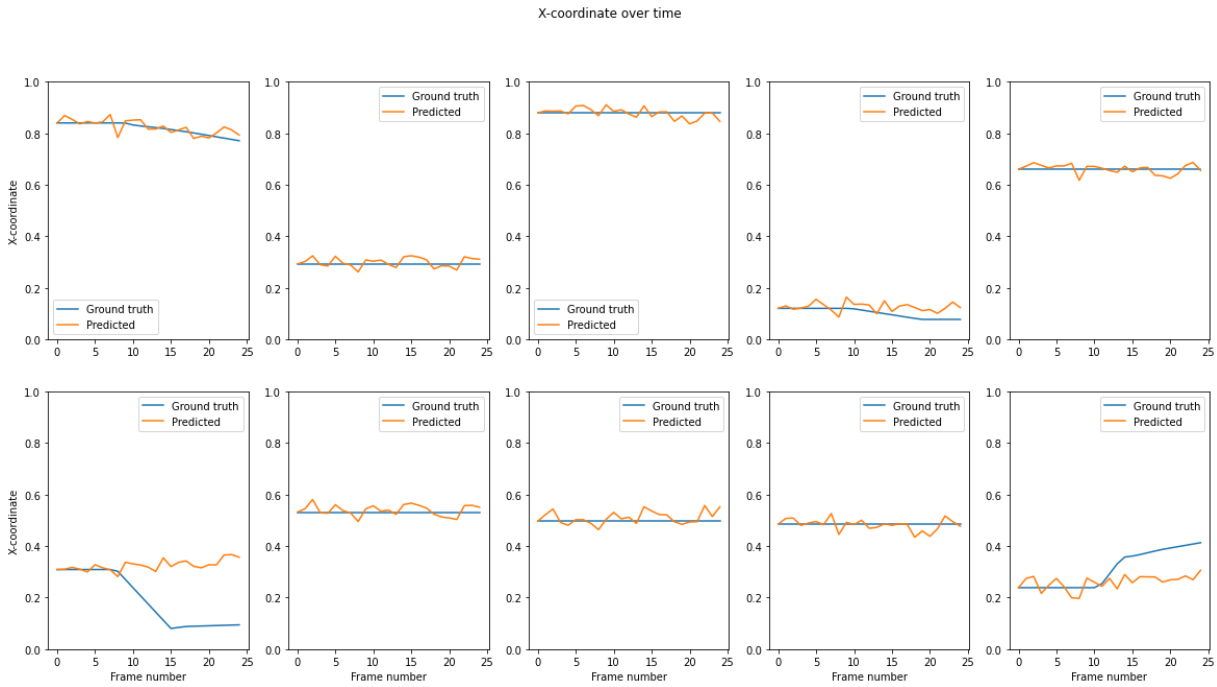

(b)

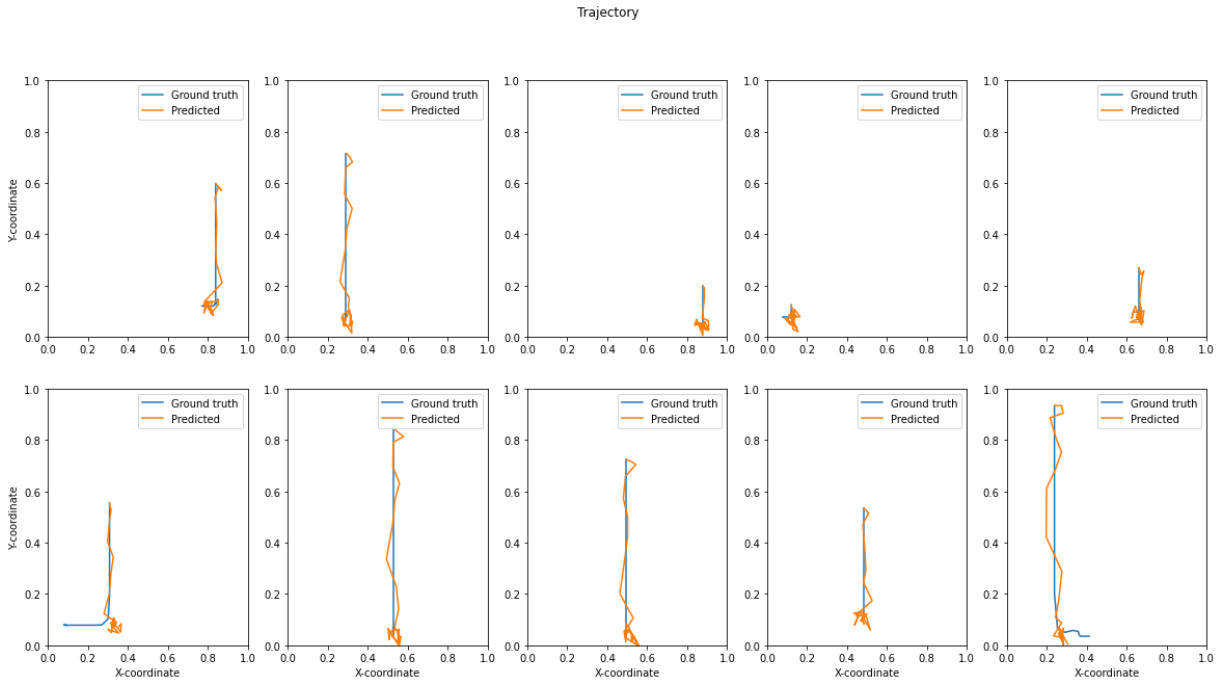

(c)

Figure 15. The first 10 test-set predictions of Vanilla RNN on scenarios with collisions. (a) Y-coordinate time series; (b) X-coordinate time series; (c) Full trajectory.

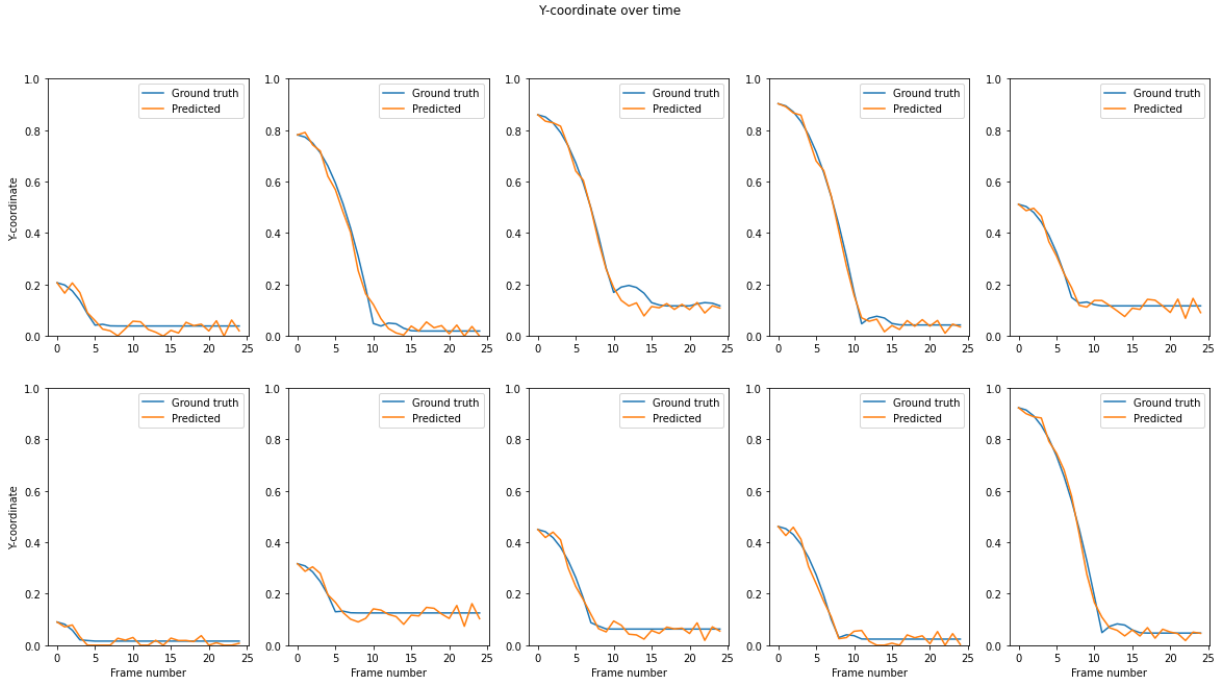
Y-coordinate over time
Ground truth
Predicted
Y-coordinate
Frame number

(a)

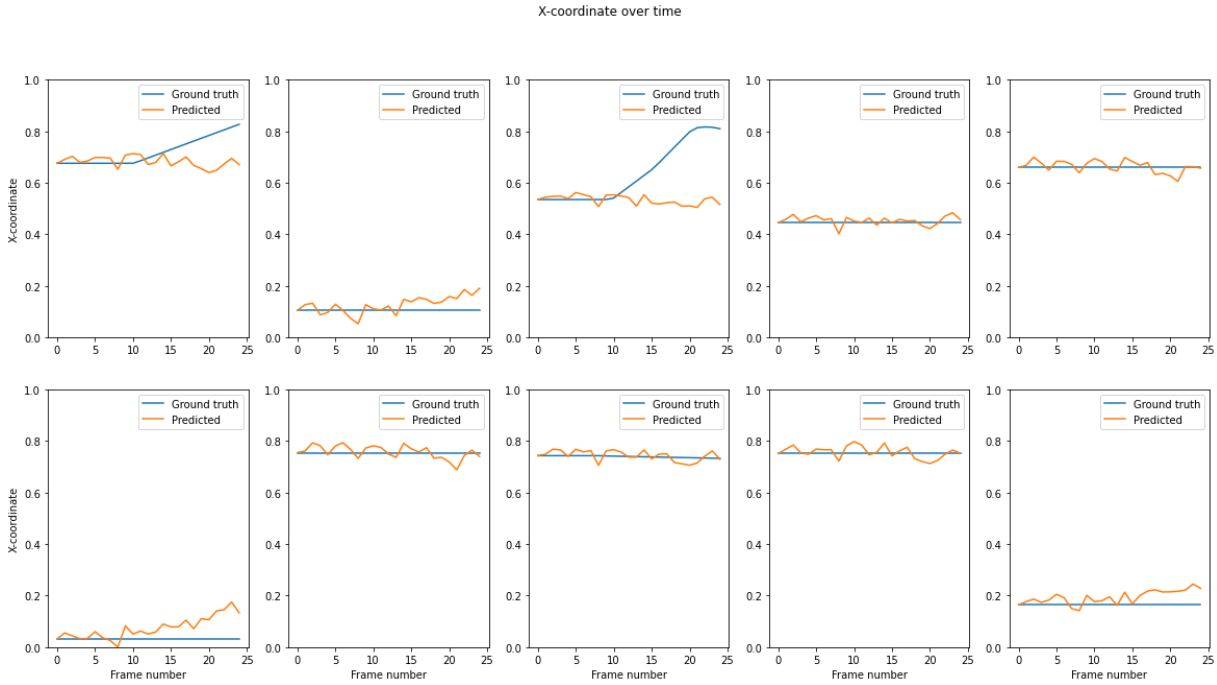
X-coordinate over time
Ground truth
Predicted
X-coordinate
Frame number

(b)

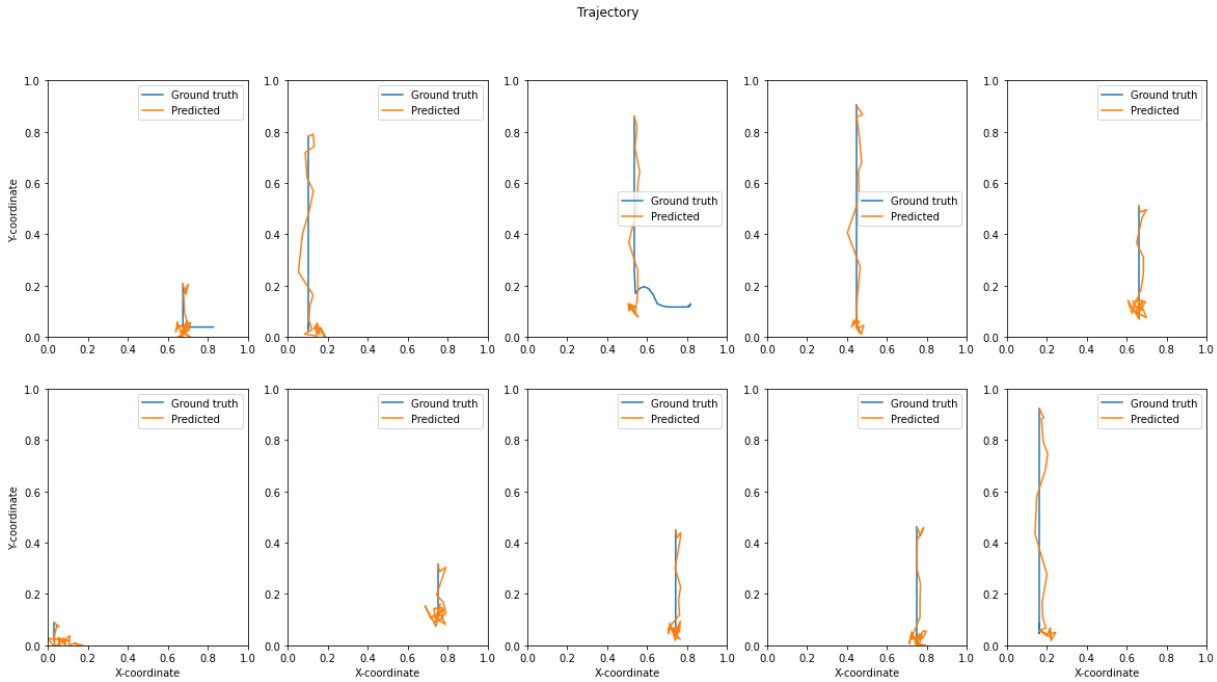

(c)

Figure 16. The first 10 test-set predictions of GRU on scenarios with collisions. (a) Y-coordinate time series; (b) X-coordinate time series; (c) Full trajectory.

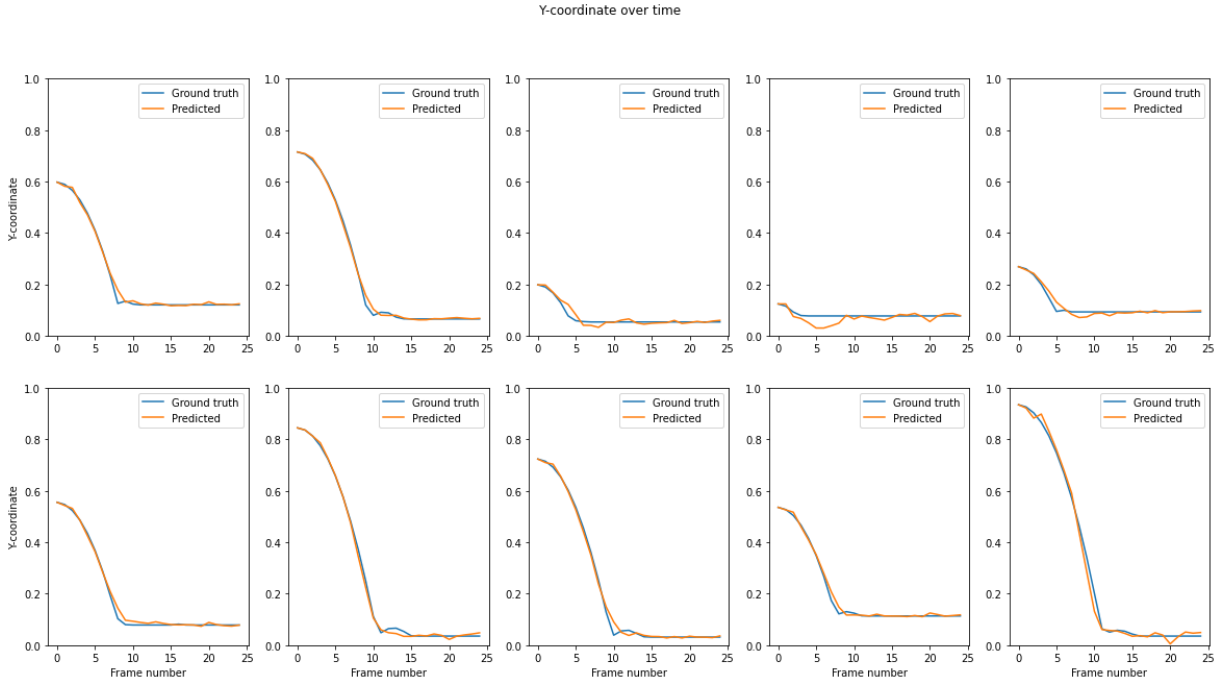
Y-coordinate over time
Ground truth
Predicted
Y-coordinate
Frame number

(a)

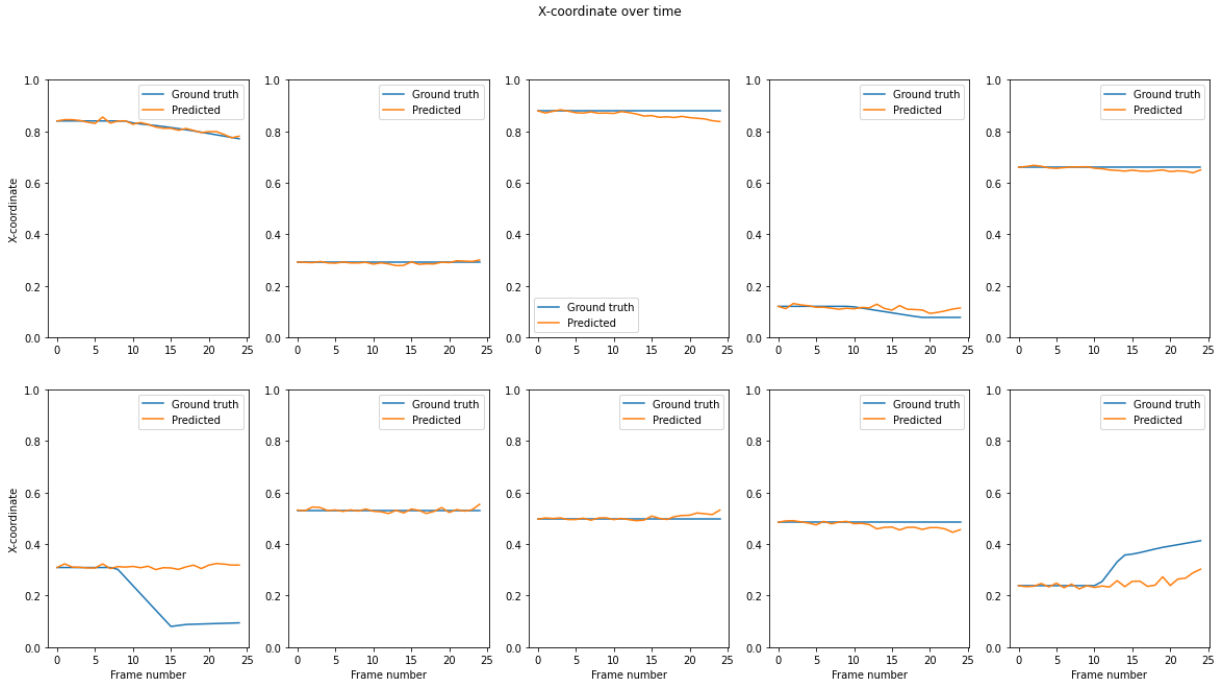
X-coordinate over time
Ground truth
Predicted
X-coordinate
Frame number

(b)

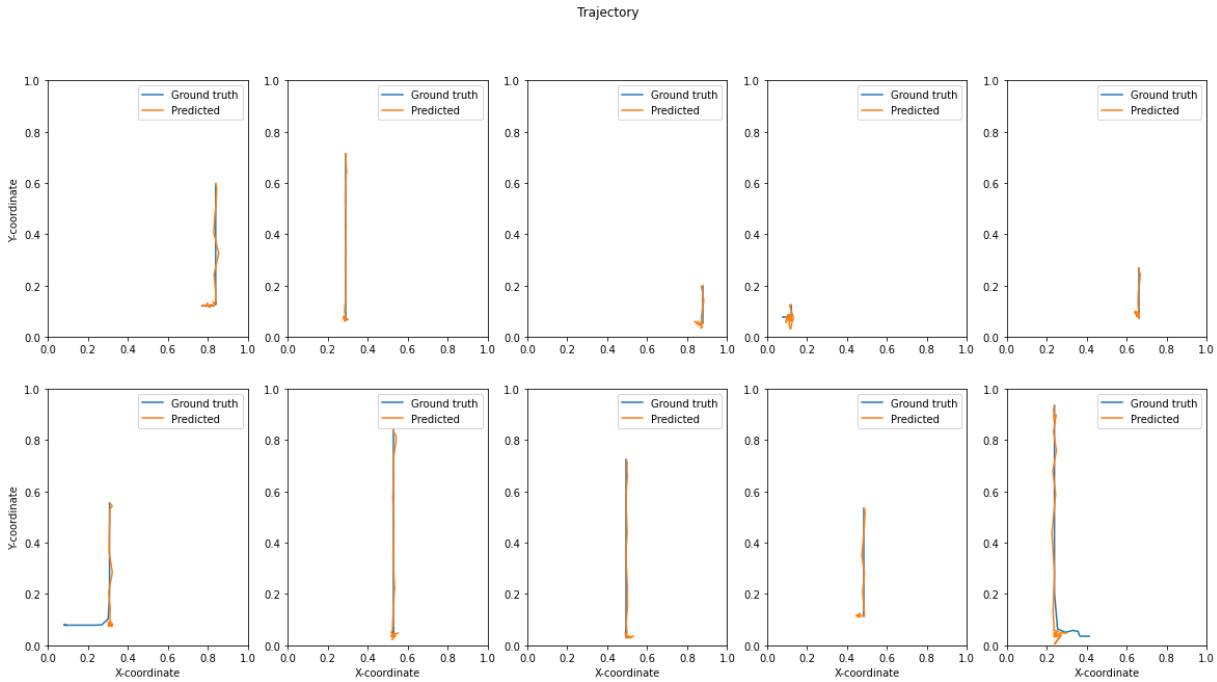

(c)

Figure 17. The first 10 test-set predictions of LSTM on scenarios with collisions. (a) Y-coordinate time series; (b) X-coordinate time series; (c) Full trajectory.

For the Reservoir Computing (RC) models, the Grid Search was performed using the following search space:

- Reservoir size: 150, 200, 250 neurons;
- Leaking rate: 0.7, 0.9;
- Spectral radius: 0.1, 0.3, 0.5;
- Ridge parameter: 0.01, 0.1.

The optimal set of hyperparameters found by Grid Search includes 200 neurons in the reservoir, a leaking rate of 0.9, a spectral radius of 0.1, and a Ridge parameter of 0.1.

I noticed that the RC models exhibit less noise in their predictions compared to traditional RNNs. However, they often incorrectly predict that the object moves upward before falling, and they also struggle to identify collisions and predict post-collision movements. The test set RMSE of RC models is shown in Table 7, which reveals that traditional RNNs provide closer predictions.

Figures 18-21 display the visualized predicted trajectories, where some of the RC models' predictions deviate significantly from the ground truth.

Model	RMSE
ESN	0.0716
Sequential ESN	0.0978
Parallel ESN	0.0741
Grouped ESN	0.1233

Table 6. RMSE of RC models on predicting trajectories with collisions from the test set.

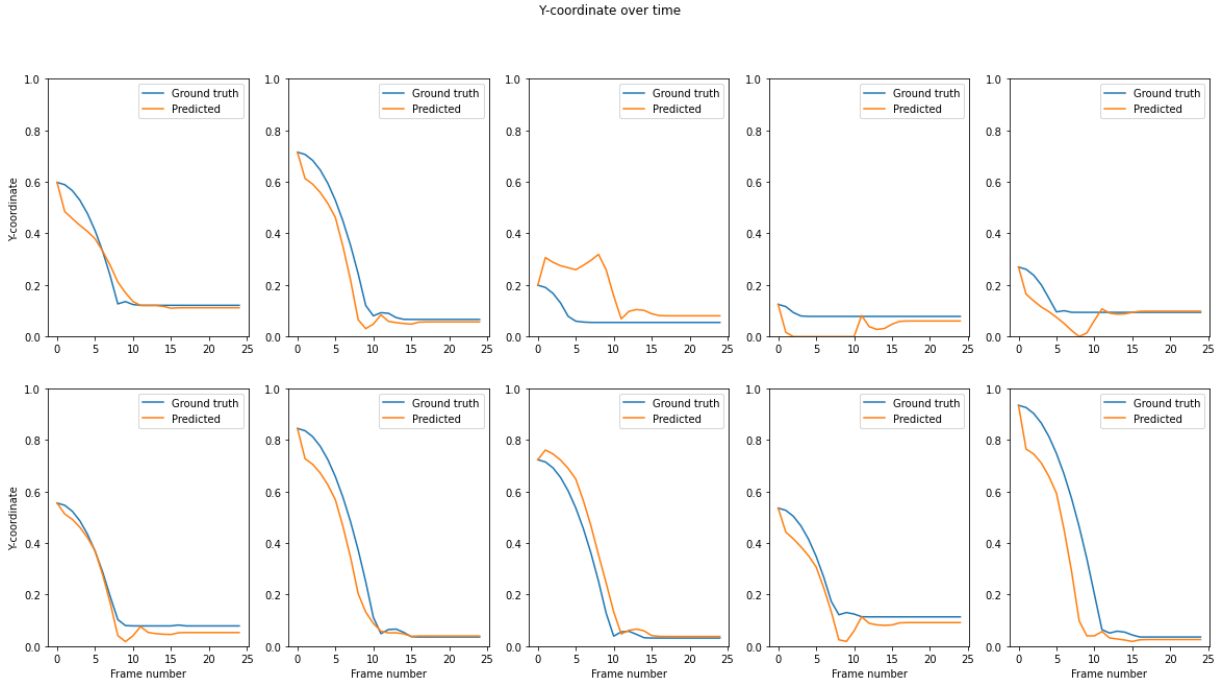

(a)

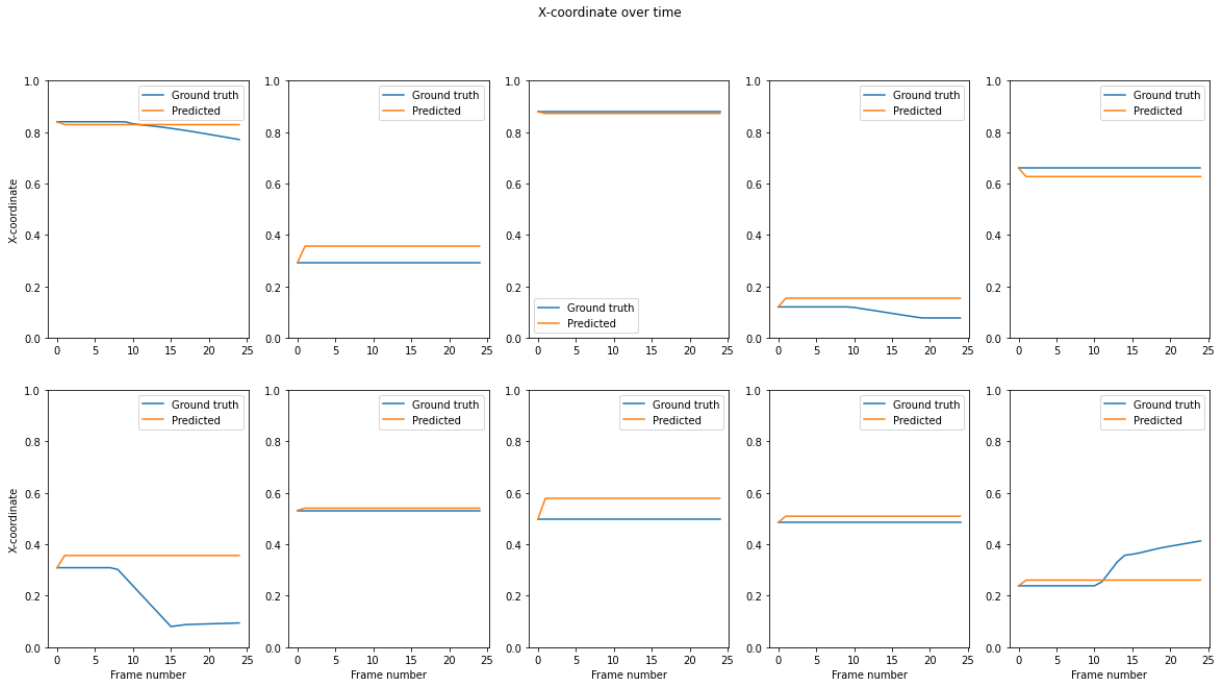

(b)

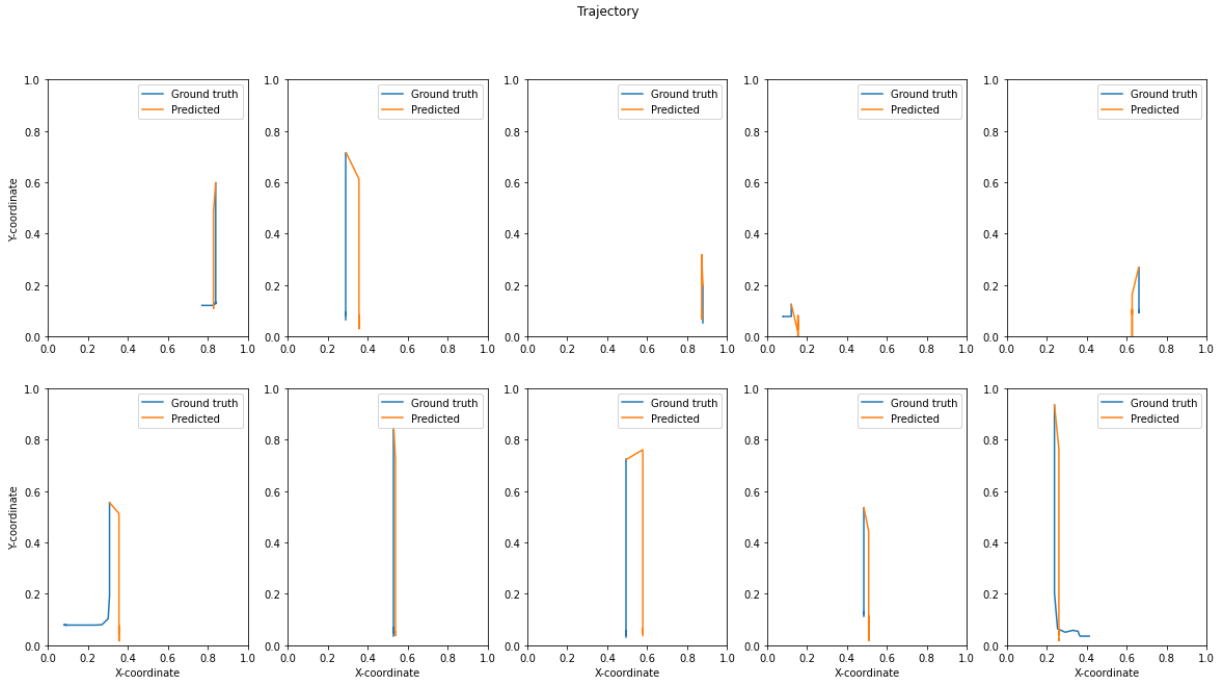

(c)

Figure 18. The first 10 test-set predictions of ESN on scenarios with collisions. (a) Y-coordinate time series; (b) X-coordinate time series; (c) Full trajectory.

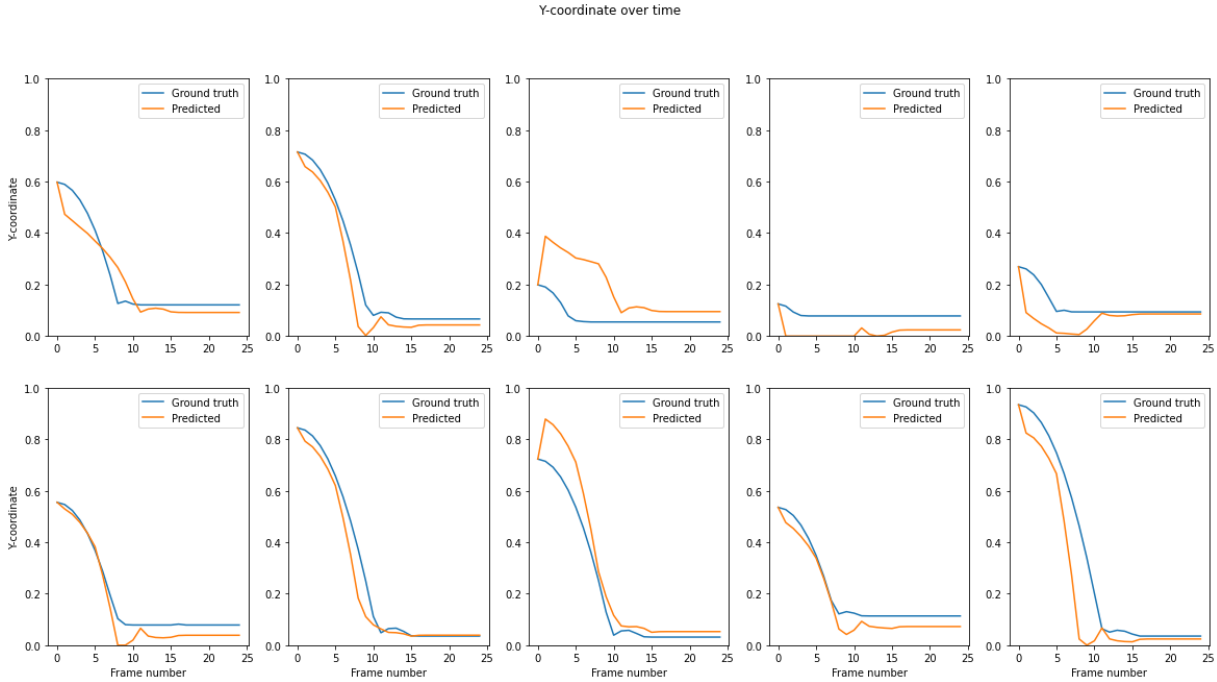
Y-coordinate over time
Ground truth
Predicted
Y-coordinate
Frame number

(a)

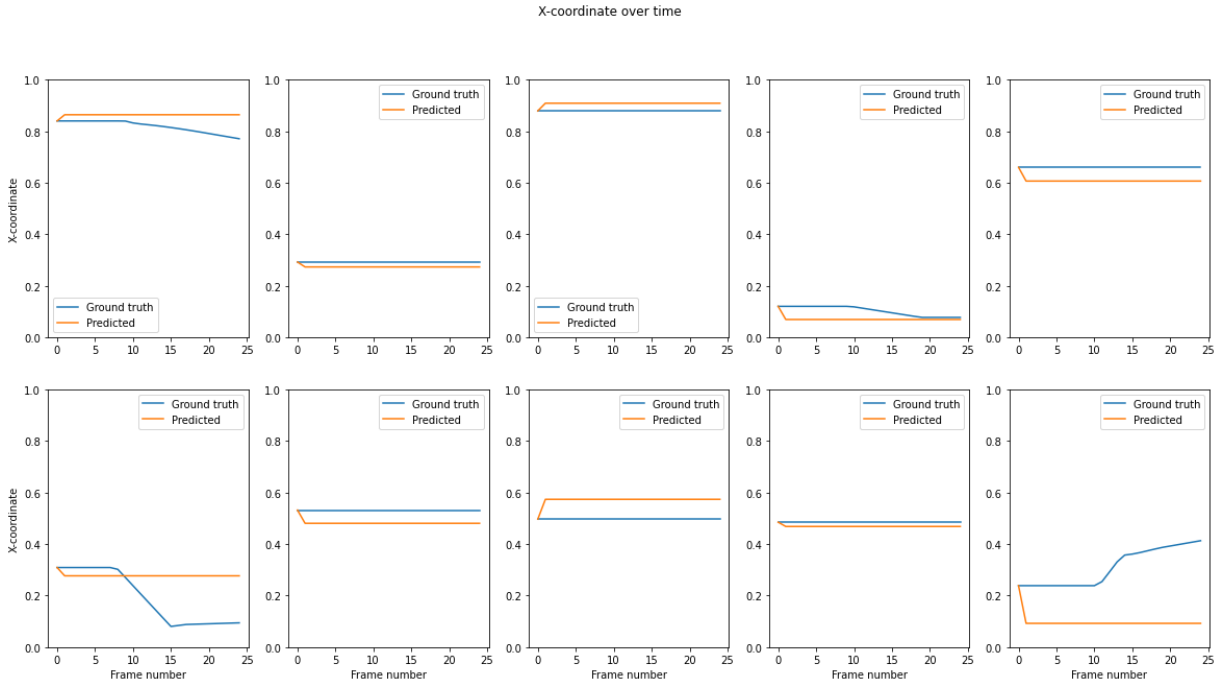
X-coordinate over time
Ground truth
Predicted
X-coordinate
Frame number

(b)

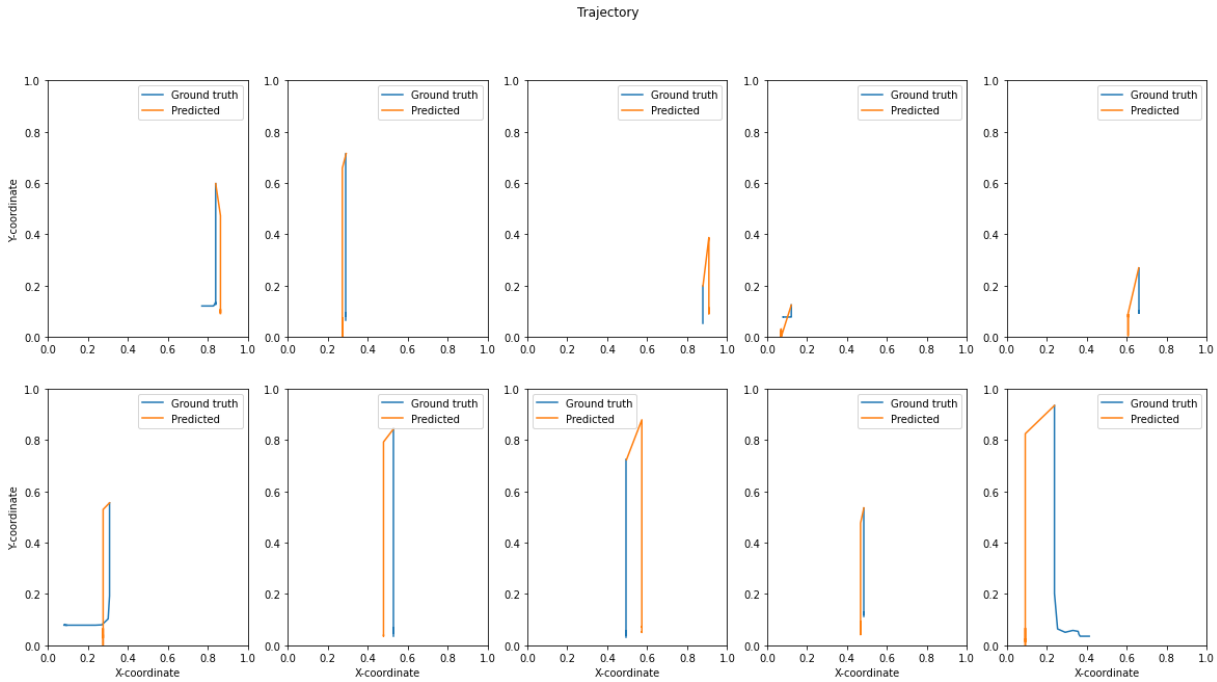

(c)

Figure 19. The first 10 test-set predictions of Sequential ESN on scenarios with collisions. (a) Y-coordinate time series; (b) X-coordinate time series; (c) Full trajectory.

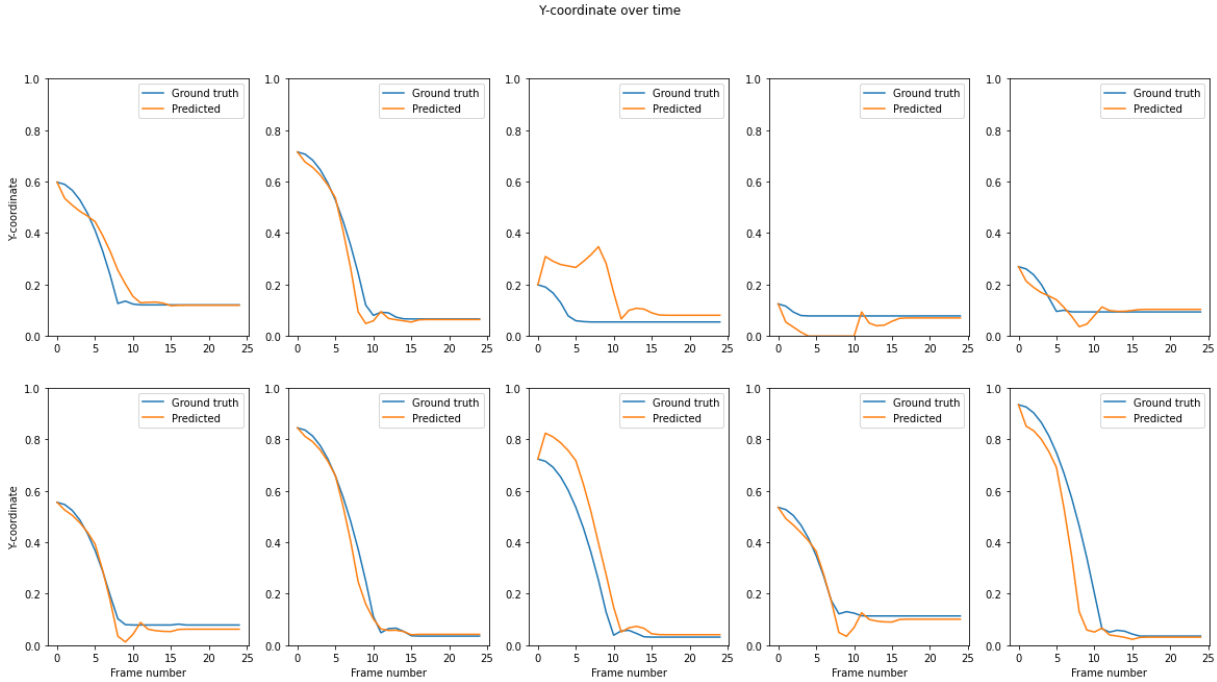
Y-coordinate over time
Ground truth
Predicted
Y-coordinate
Frame number

(a)

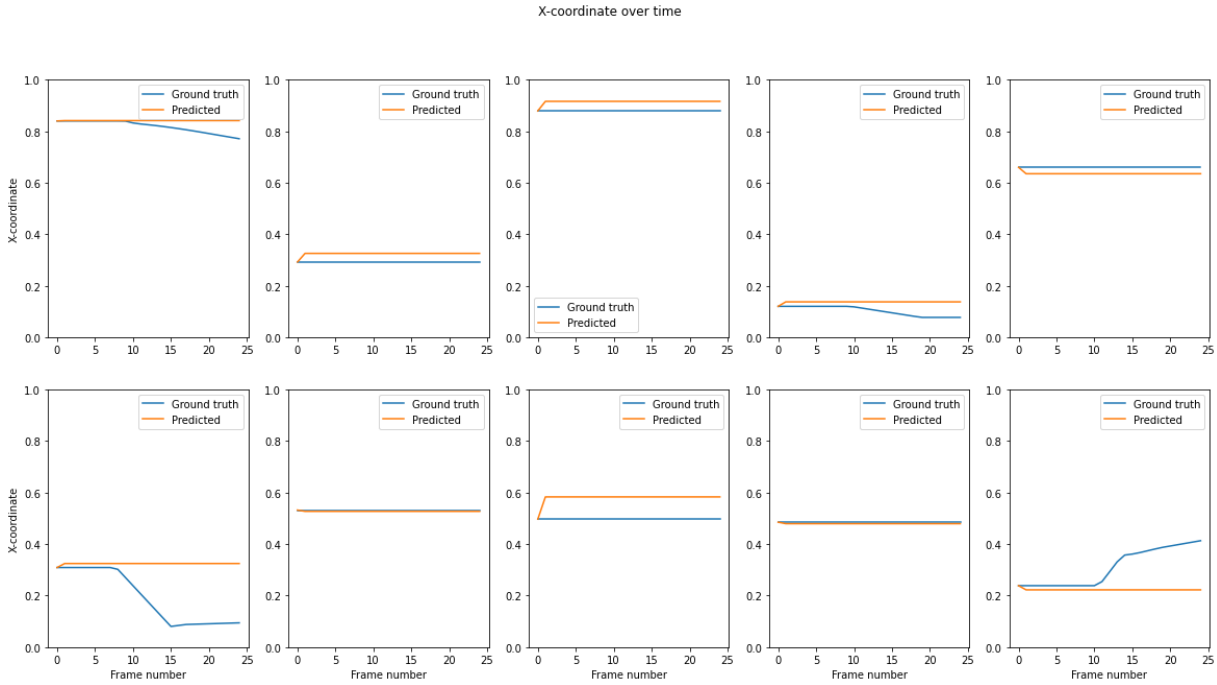
X-coordinate over time
Ground truth
Predicted
X-coordinate
Frame number

(b)

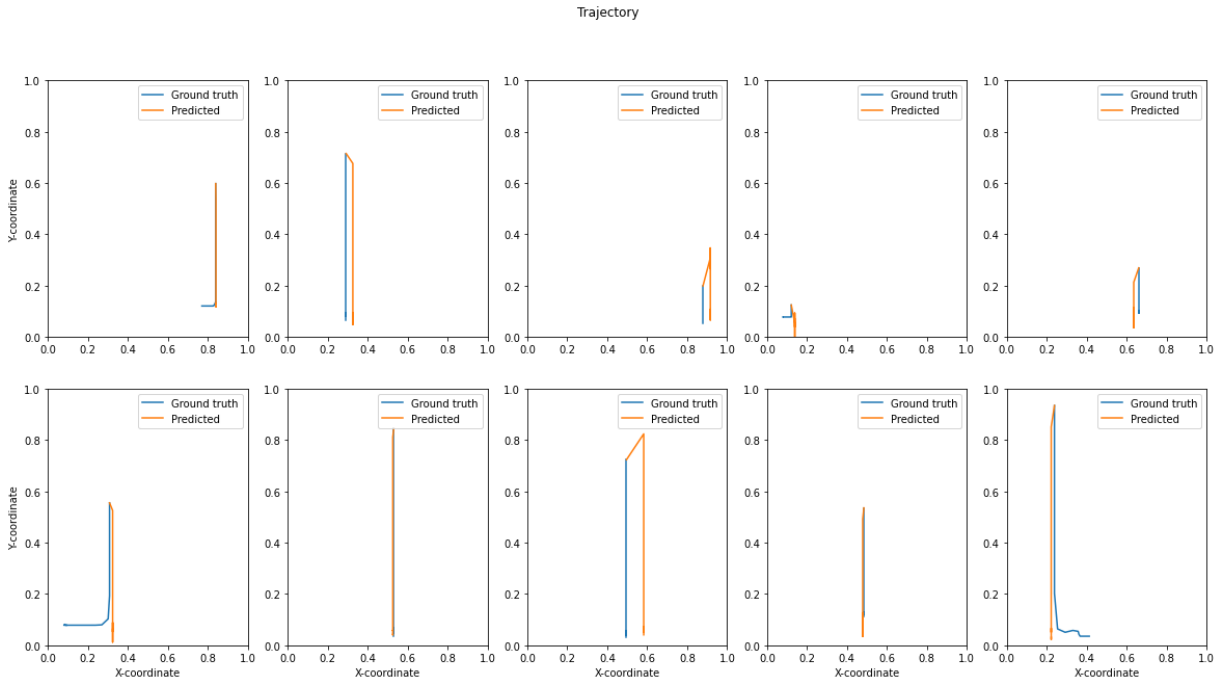

(c)

Figure 20. The first 10 test-set predictions of Parallel ESN on scenarios with collisions. (a) Y-coordinate time series; (b) X-coordinate time series; (c) Full trajectory.

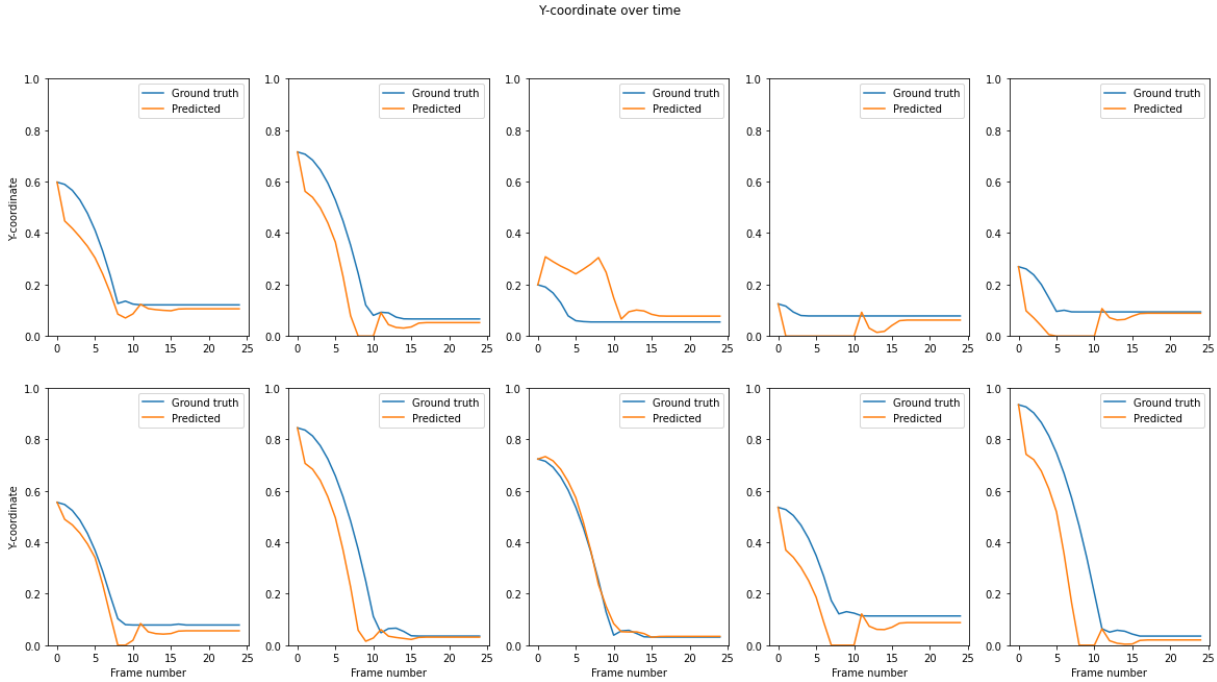
Y-coordinate over time
Ground truth
Predicted
Y-coordinate
Frame number

(a)

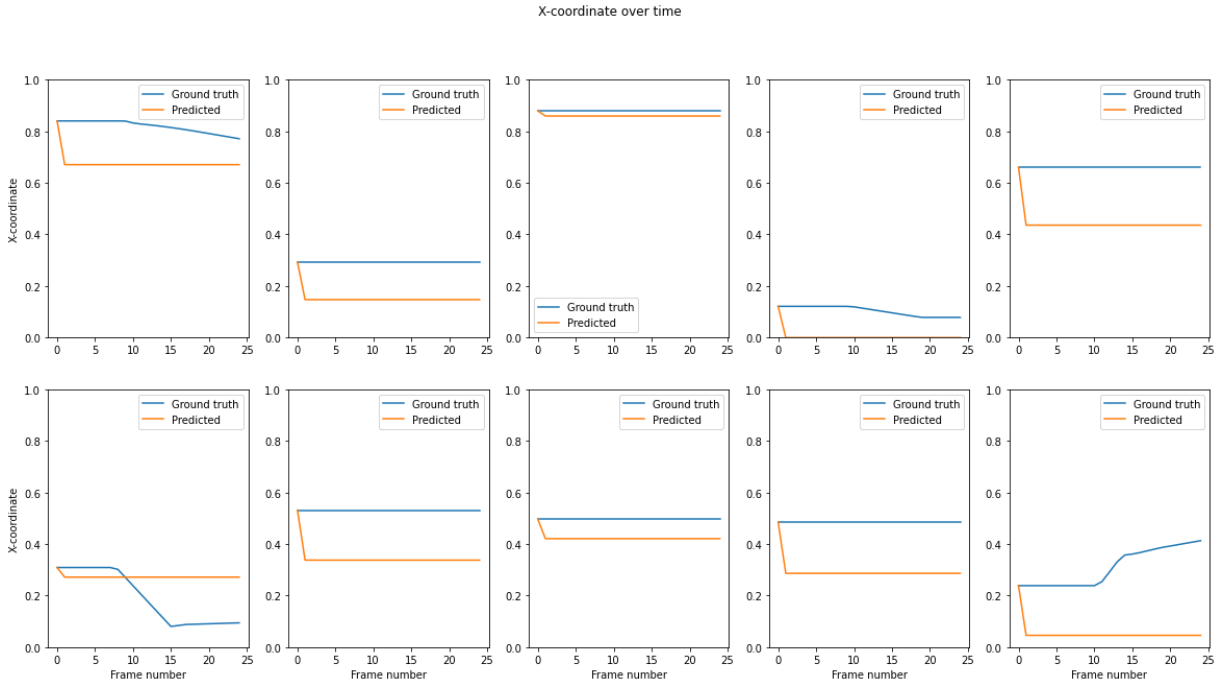
X-coordinate over time
Ground truth
Predicted
X-coordinate
Frame number

(b)

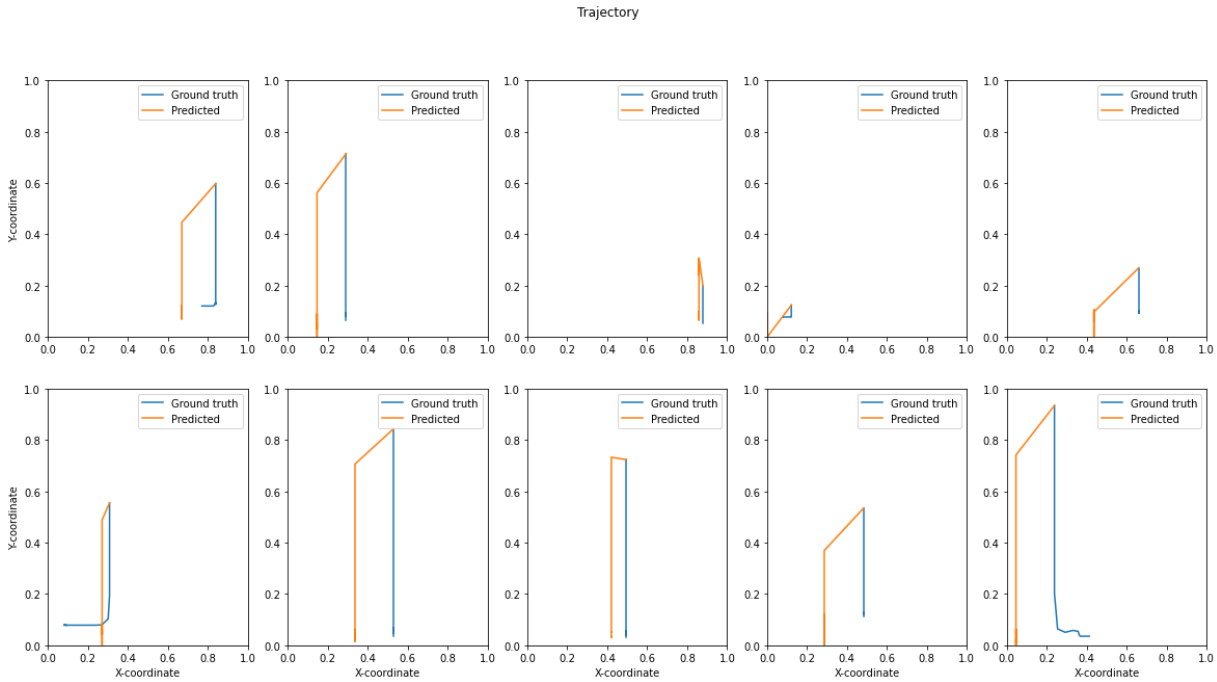

(c)

Figure 21. The first 10 test-set predictions of Grouped ESN on scenarios with collisions. (a) Y-coordinate time series; (b) X-coordinate time series; (c) Full trajectory.

In conclusion, both traditional RNNs and RC models face challenges in predicting trajectories with collisions. While traditional RNNs generate closer predictions, both model types struggle to accurately predict collisions and post-collision movements. Further research is needed to improve the performance of these models in complex scenarios involving collisions.

5.3. Predicting the evolution of the entire scene

As an extension task, I trained the models with the goal to predict the movement of all three balls simultaneously, instead of focusing on just one ball. This involves predicting 144 values (x- and y-coordinates of 3 balls on 24 simulation frames) instead of 48 values (x- and y-coordinates of only a single ball on 24 simulation frames).

For the traditional RNNs, I started with the Grid Search again, using the same search space as before. The optimal hyperparameters were found to be 128 hidden neurons, 2 recurrent layers,

and 0 dropout rate for LSTM and GRU, and 3 recurrent layers, 128 hidden neurons, and 0 dropout rate for Vanilla RNN.

The test set RMSE for the traditional models is given in Table 7. Surprisingly, the RMSE was found to be approximately the same as for the single-ball trajectory prediction with collisions, even though the number of predicted values increased threefold. This means the error per predicted value was three times smaller. However, the visual assessment of the results did not show significant improvements; the models still failed to accurately predict the trajectories of the balls. Figures 22-24 show the predicted and ground truth trajectories of each ball and the entire scene evolution done by traditional RNN models on the test set.

Model	**RMSE**
Vanilla RNN	0.0494
GRU	0.0466
LSTM	0.0460

Table 7. RMSE of traditional models on predicting the scene evolution using the data from the test set.

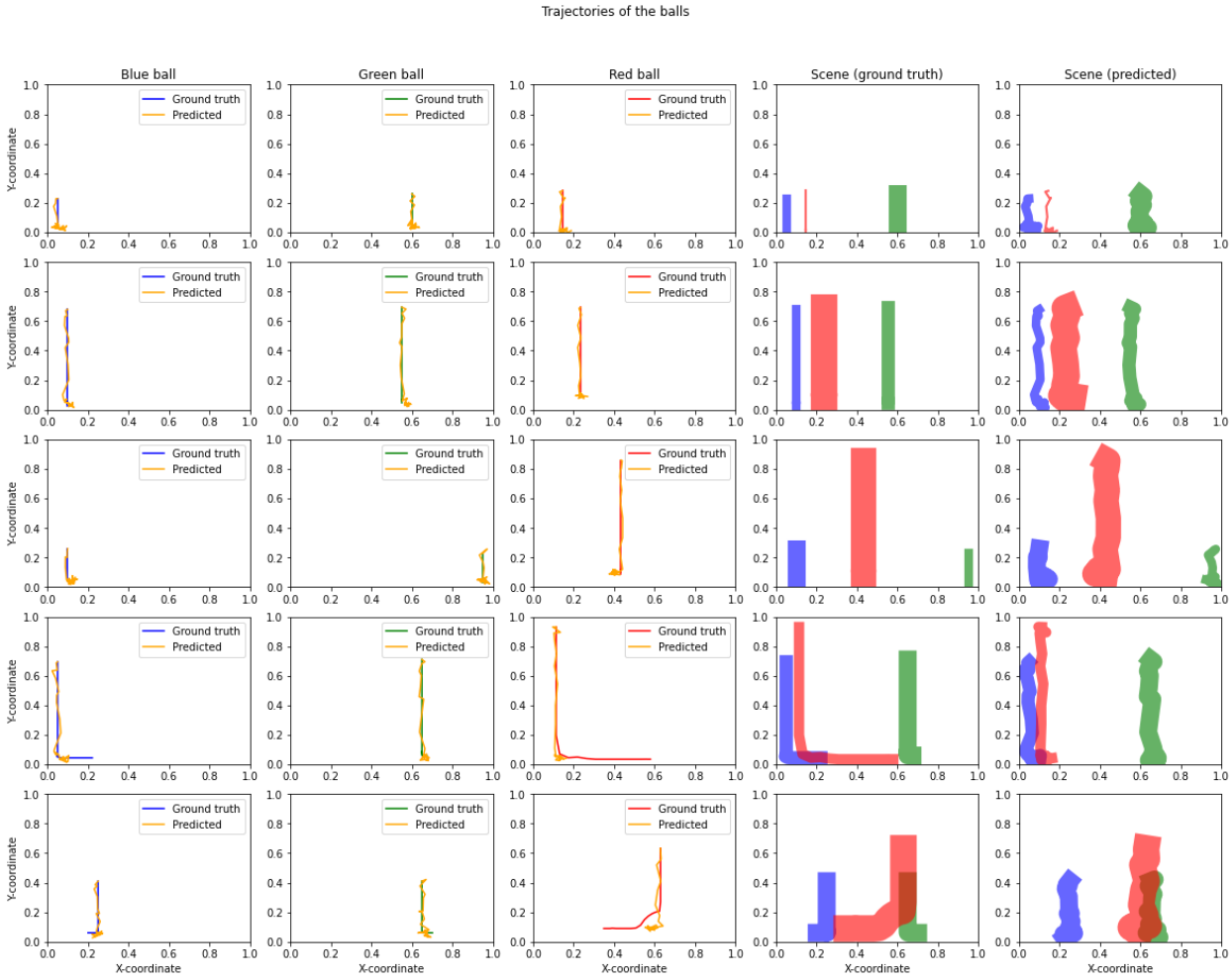

Figure 22. First 5 predicted and ground-truth trajectories of each ball, ground-truth, and predicted scene evolution done by Vanilla RNN on the test set.

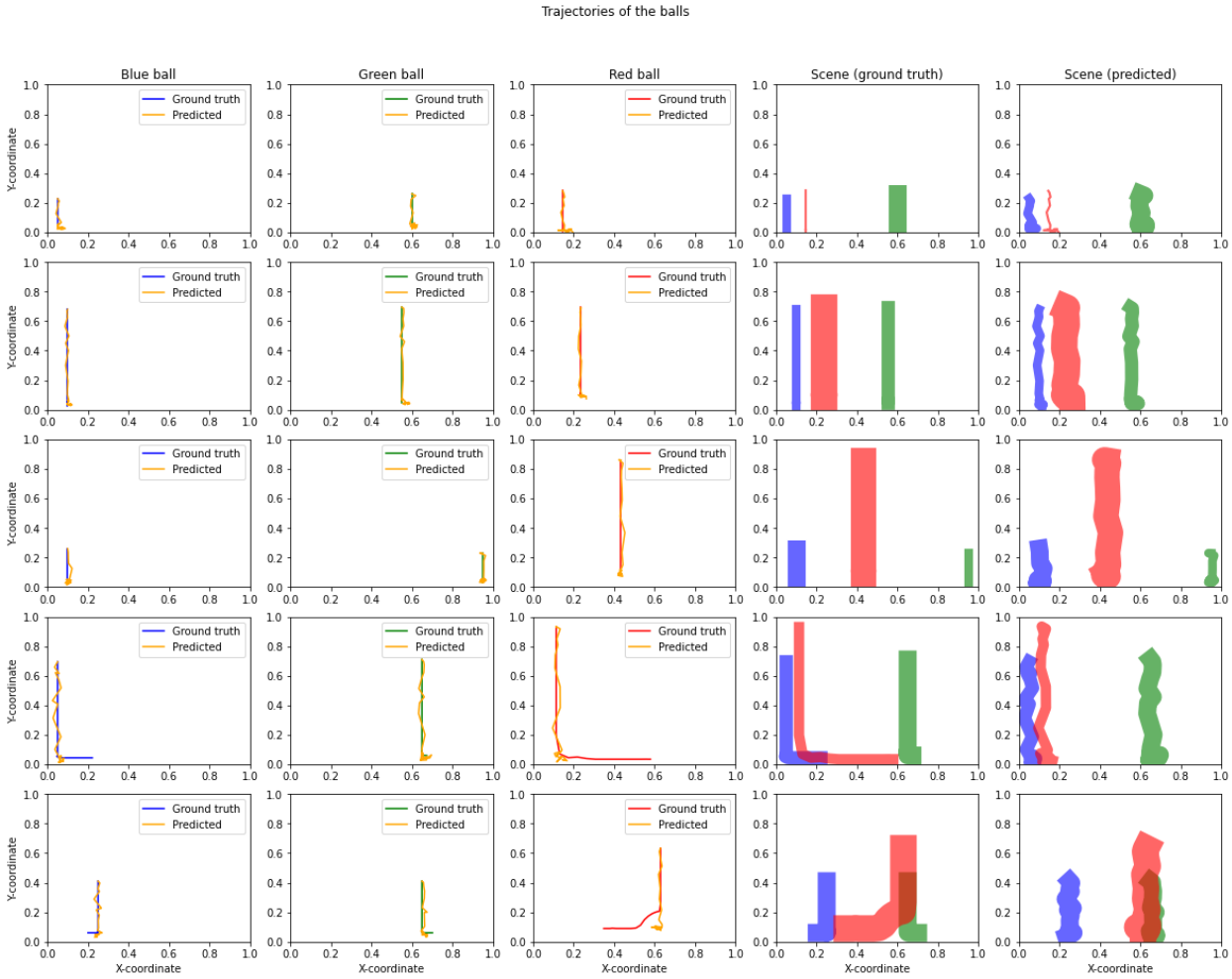

Figure 23. First 5 predicted and ground-truth trajectories of each ball, ground-truth, and predicted scene evolution done by GRU on the test set.

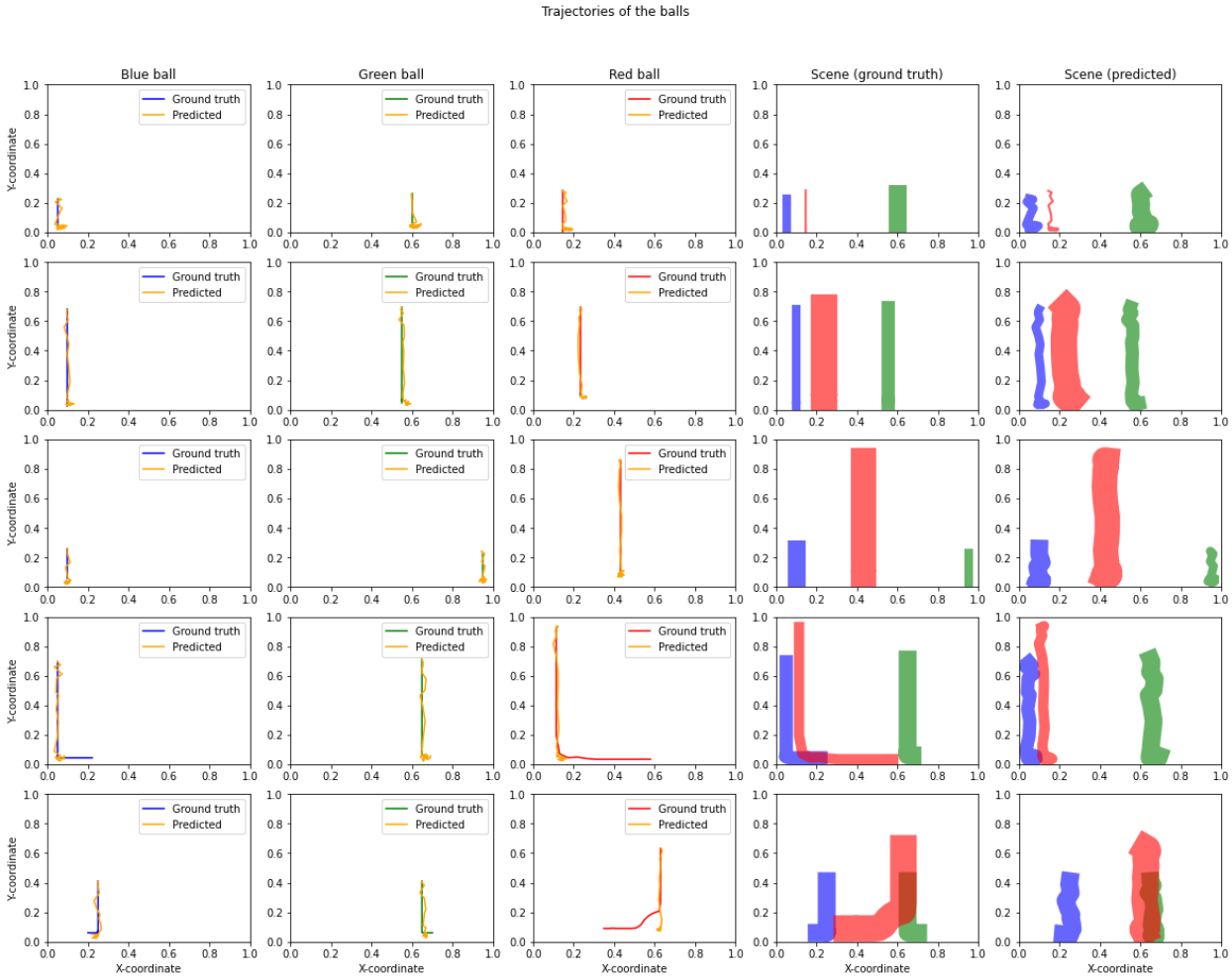

Figure 24. First 5 predicted and ground-truth trajectories of each ball, ground-truth, and predicted scene evolution done by LSTM on the test set.

For the RC models, I changed the search space to

- Reservoir size: 200, 250, 300, 350
- Leaking rate: 0.7, 0.9
- Spectral radius: 0.1, 0.3, 0.5
- Ridge parameter: 0.01, 0.1

This change was motivated by my assumption that a more complicated task would require a larger reservoir size. The optimal set of hyperparameters that was found by Grid Search is 300

neurons in a reservoir, a leaking rate of 0.9, a spectral radius of 0.3, and a Ridge parameter of 0.1.

The test set prediction error for each RC model is shown in Table 8. These errors were significantly larger than those of the traditional RNN models for the same task. However, the visual assessment revealed an advantage of the RC models: for incorrectly predicted collisions, they still reasonably predicted the movement of the balls caused by such collisions. This effect was most prominent in the visualizations of the predicted scene evolutions done by the Parallel ESN model. Figures 25-28 show the ground truth and predicted trajectories of each ball, along with the ground truth and predicted scene evolution made by each RC model using the test set.

Model	**RMSE**
ESN	0.1867
Sequential ESN	0.2160
Parallel ESN	0.2176
Grouped ESN	0.1898

Table 8. RMSE of RC on predicting the scene evolution using the data from the test set.

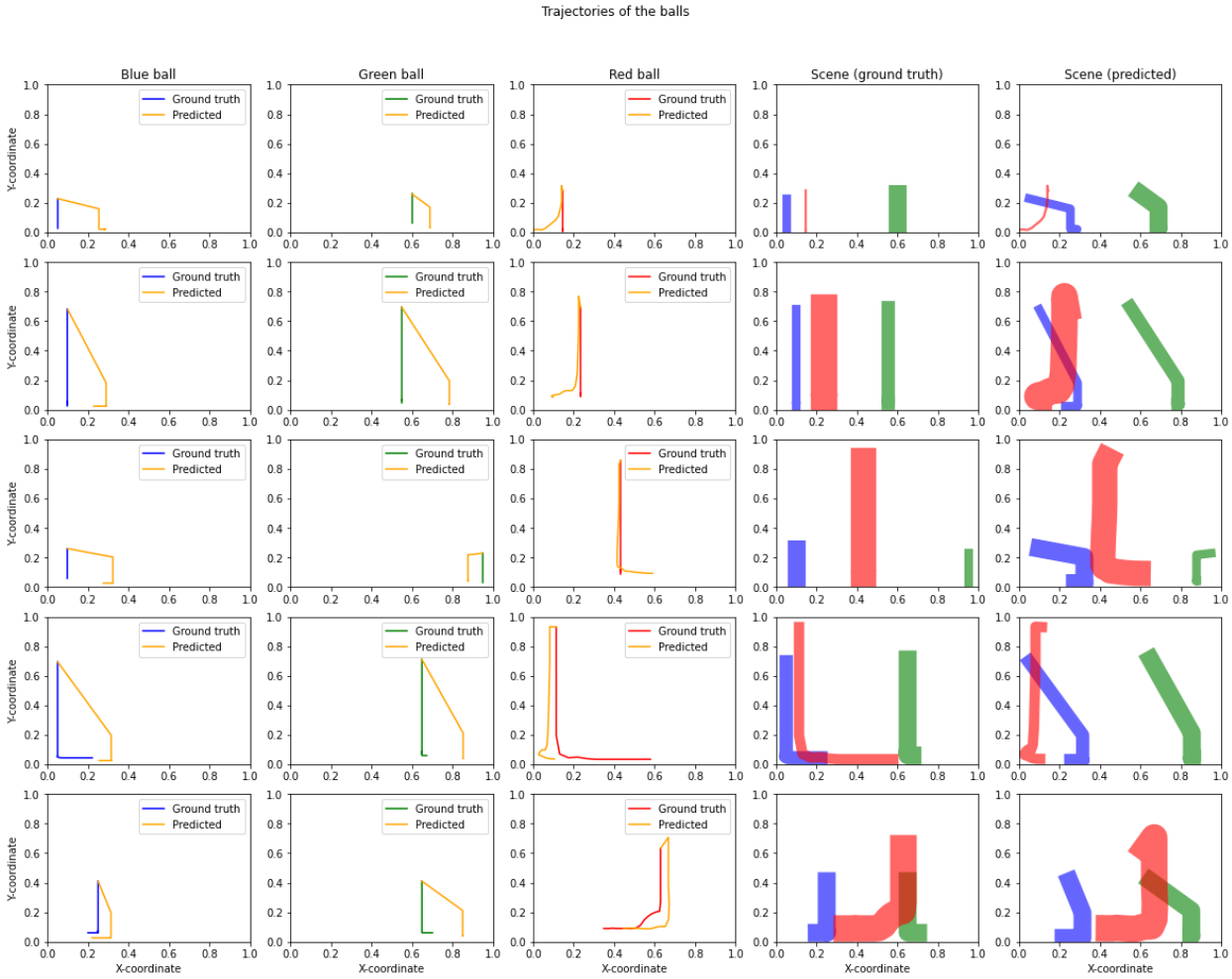

Figure 25. The first 5 predicted and ground-truth trajectories of each ball, ground-truth, and predicted scene evolution done by simple ESN on the test set.

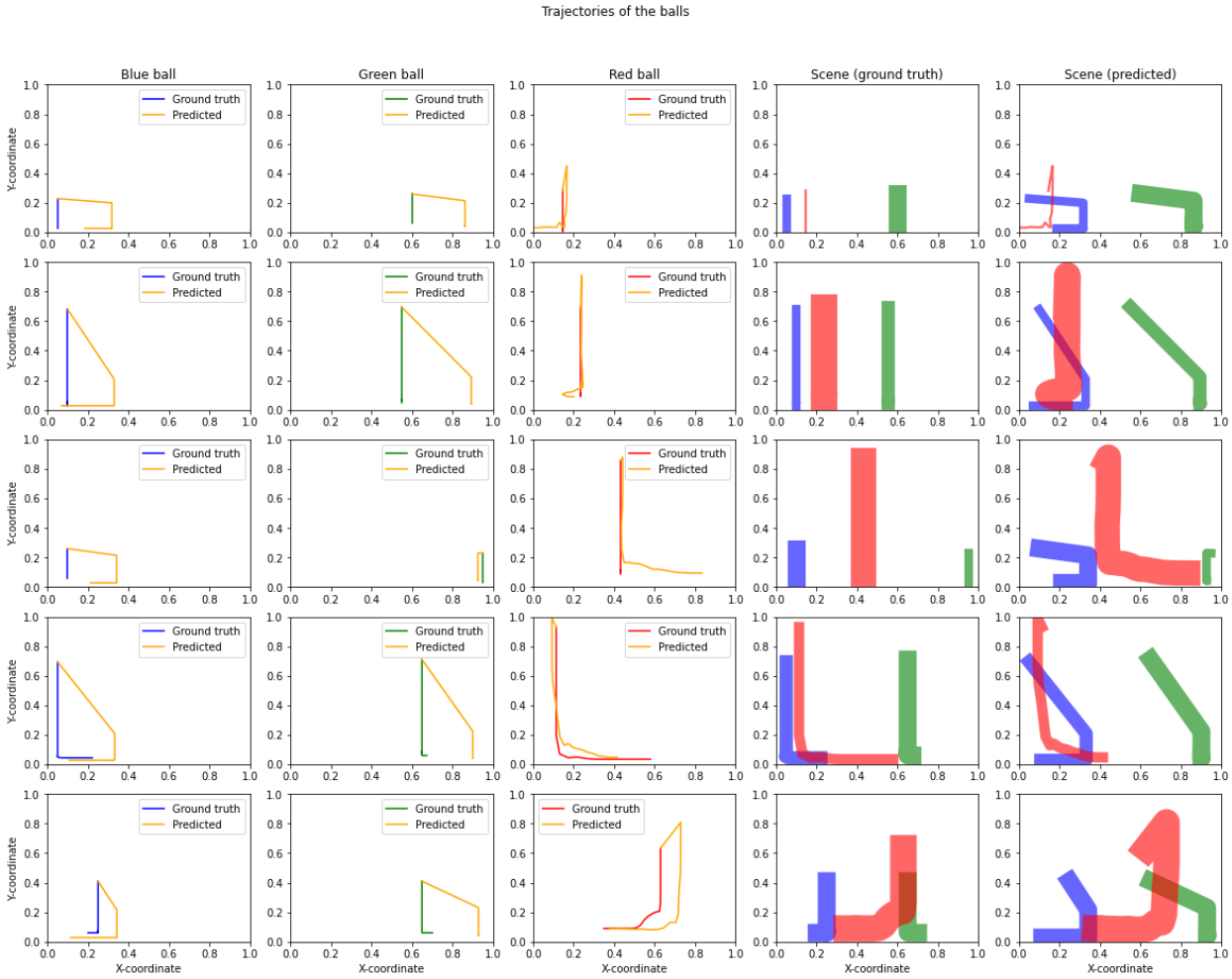

Figure 26. The first 5 predicted and ground-truth trajectories of each ball, ground-truth, and predicted scene evolution done by Sequential ESN on the test set.

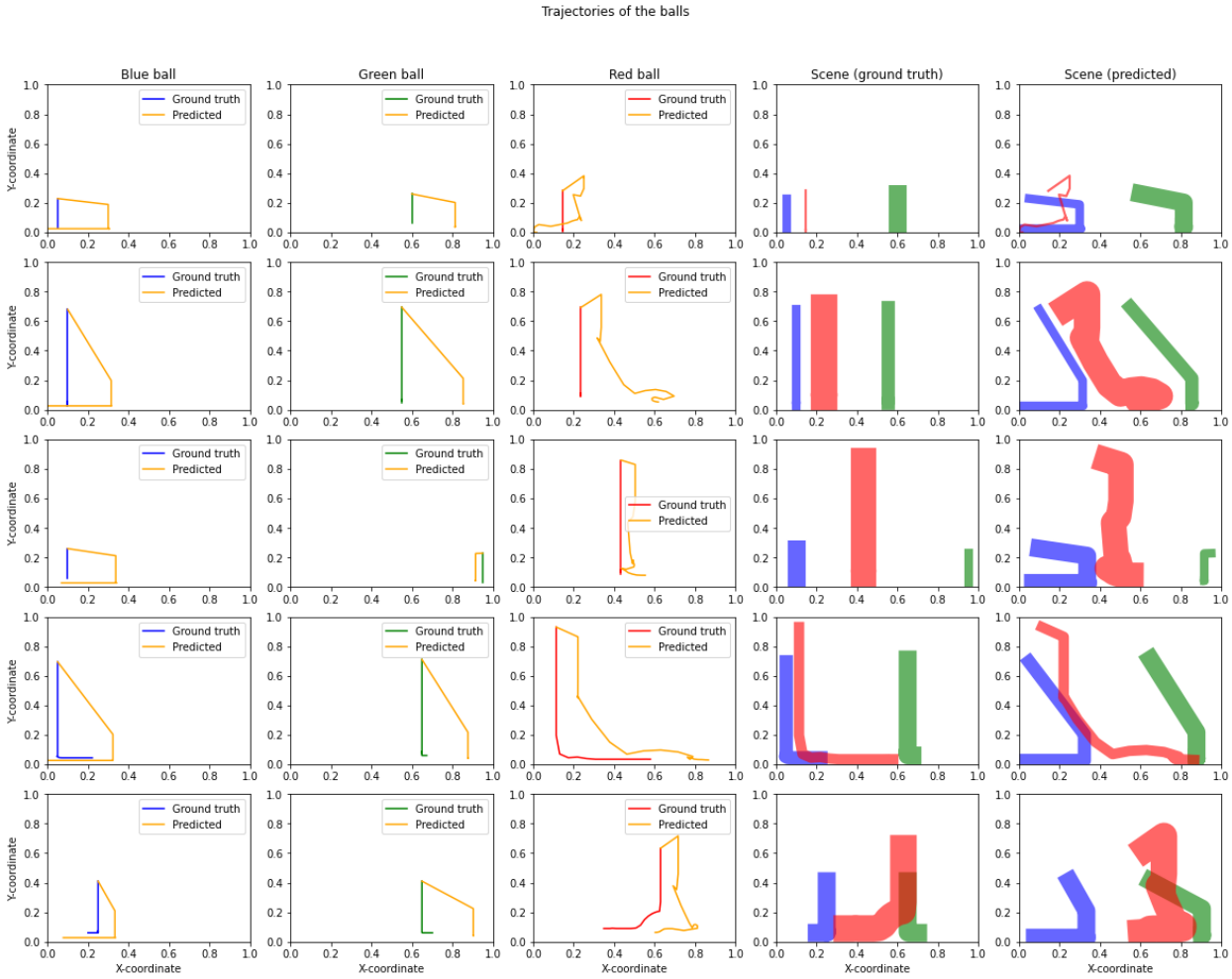

Figure 27. The first 5 predicted and ground-truth trajectories of each ball, ground-truth, and predicted scene evolution done by Parallel ESN on the test set.

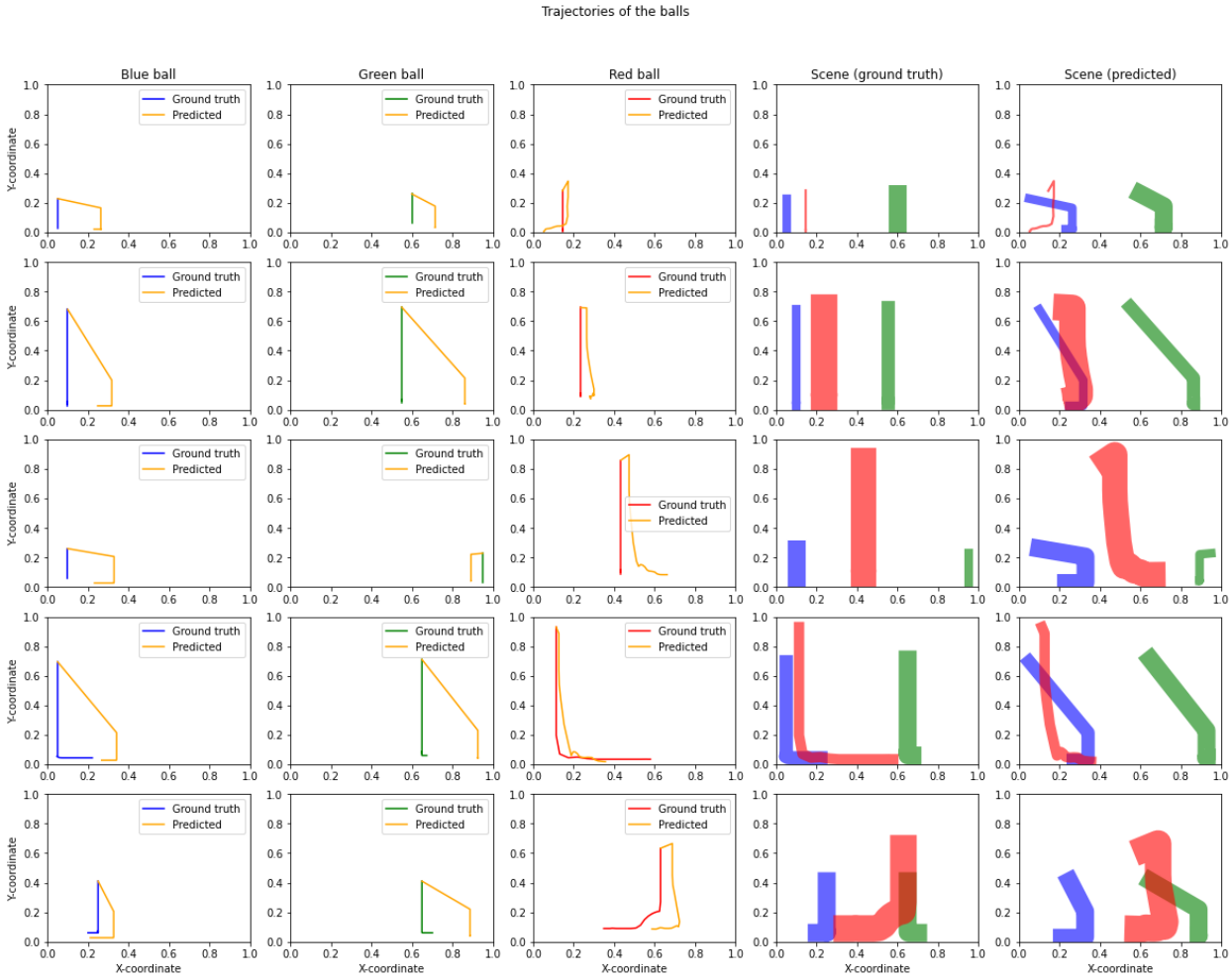

Figure 28. The first 5 predicted and ground-truth trajectories of each ball, ground-truth, and predicted scene evolution done by Grouped ESN on the test set.

In summary, traditional RNN models performed better in terms of RMSE on predicting the entire scene evolution, but RC models demonstrated the ability to reasonably predict the movement of balls for incorrectly predicted collisions. Both model types still struggled to accurately predict the trajectories of the balls and further improvements are needed.

Section 6. Conclusion and Future Work

In this Capstone Project, I investigated the performance of traditional Recurrent Neural Networks (RNNs) and Reservoir Computing (RC) models in predicting the trajectory of a ball in a simulated 2D environment. My primary focus was on comparing the performance of Vanilla RNN, Gated Recurrent Unit (GRU), Long Short-Term Memory (LSTM), Echo State Network (ESN), and its deep variations (Sequential ESN, Parallel ESN, and Grouped ESN) in three different tasks: predicting free-fall trajectories, predicting single-ball trajectories with collisions, and predicting the evolution of the entire scene with three balls.

For the task of predicting free-fall trajectories, all models showed satisfactory results, with LSTM and GRU models achieving the best performance. In the more complex task of predicting single-ball trajectories with collisions, the performance of all models decreased, but LSTM demonstrated the least noisy predictions. For Reservoir Computing models, the amount of noise in predictions was drastically less, but they were less accurate than traditional RNN models.

In the extension task of predicting the evolution of the entire scene, traditional RNN models showed surprisingly better results compared to single-ball trajectory prediction with collisions. Despite the increase in the number of predicted values, the error per predicted value was three times smaller. On the other hand, while RC models' error rates were higher than traditional RNNs, they demonstrated an ability to reasonably predict the movement of balls for incorrectly predicted collisions.

My study highlights the strengths and weaknesses of traditional RNNs and RC models in predicting complex ball trajectories in a 2D environment. Traditional RNNs, particularly LSTM and GRU, showed better overall performance, but RC models demonstrated some advantages in specific situations, such as predicting the movement of balls in incorrectly predicted collisions. While both model types struggled to accurately predict ball trajectories in complex scenarios,

this research provides valuable insights into the capabilities of RNNs and RC models for trajectory prediction tasks and potential improvements that can be made for future studies. **Obtained results allow me to speculate the conclusion that Reservoir Computing models are doing a better job learning the underlying physics compared to traditional RNNs but struggle to make accurate predictions.**

Future work can focus on expanding the complexity of the simulated environment by including more objects on the scene, introducing different types of objects (e.g., different shapes and static objects), transitioning to a 3D environment, and ultimately using real-world data to validate the models' performance. These directions would allow for a more comprehensive understanding of the models' capabilities in predicting trajectories in more realistic and diverse scenarios.

Throughout the course of this project, I gained valuable experience and skills in several aspects of machine learning and deep learning research. I learned how to use PyTorch to architect and train deep learning models effectively. I also developed the ability to manipulate data and prepare it for usage with PyTorch, ensuring that the models receive the appropriate input for training and evaluation. I discovered the importance of heuristics in gaining insights into the data and how they can help guide the choice of an appropriate model for a given problem. Additionally, I developed a deeper understanding of hyperparameters and how to optimize them through techniques like Grid Search, which is essential for enhancing the performance of machine learning models.

Furthermore, I delved into the world of Echo State Networks, learning about their unique architecture and how to implement them using the Reservoirpy framework. This exploration allowed me to appreciate the potential benefits and limitations of Reservoir Computing models in comparison to traditional RNNs. Lastly, I applied a bottom-up approach to research, which involved starting with simple scenarios and gradually increasing complexity, to better understand the strengths and weaknesses of the models under study.

This Capstone Project has provided me with a solid foundation in machine learning and deep learning techniques, and the insights gained from this research will undoubtedly be beneficial in my future endeavors in the field of Artificial Intelligence.

References

Bakhtin, A., van der Maaten, L., Johnson, J., Gustafson, L., & Girshick, R. (2019, August 15). *PHYRE: A new benchmark for physical reasoning*. arXiv.org. Retrieved from https://arxiv.org/abs/1908.05656

Bengio, Y., Simard, P., & Frasconi, P. (1994, March). *Learning long-term dependencies with gradient descent is ... - IEEE xplore*. IEEEXplore. Retrieved from https://ieeexplore.ieee.org/document/279181

Malik, Z. K., Hussain, A., & Wu, Q. M. J. (2016, June). *Multilayered echo state machine: A novel architecture and algorithm*. Retrieved from https://www.researchgate.net/publication/304192098_Multilayered_Echo_State_Machine_A_Novel_Architecture_and_Algorithm

Mottaghi, R., Bagherinezhad, H., Rastegari, M., & Farhadi, A. (2015, November 12). *Newtonian image understanding: Unfolding the dynamics of objects in Static Images*. arXiv.org. Retrieved from https://arxiv.org/abs/1511.04048

Mottaghi, R., Rastegari, M., Gupta, A., & Farhadi, A. (2016, March 17). *"What happens if..." Learning to predict the effect of forces in images*. arXiv.org. Retrieved from https://arxiv.org/abs/1603.05600

Lukosevicius, M. (2012). *A practical guide to applying Echo State Networks*. Retrieved from https://www.ai.rug.nl/minds/uploads/PracticalESN.pdf

Pascanu, R., Mikolov, T., & Bengio, Y. (2013, May 26). On the difficulty of training recurrent neural networks. PMLR. Retrieved from https://proceedings.mlr.press/v28/pascanu13.html

Paszke, A., Gross, S., Massa, F., Lerer, A., Bradbury, J., Chanan, G., … Chintala, S. (2019). PyTorch: An Imperative Style, High-Performance Deep Learning Library. In *Advances in Neural Information Processing Systems 32* (pp. 8024–8035). Curran Associates, Inc.

Retrieved from http://papers.neurips.cc/paper/9015-pytorch-an-imperative-style-high performance-deep-learning-library.pdf

Song, Z., Wu, K., & Shao, J. (2020, April 12). *Destination prediction using Deep Echo State Network*. Retrieved from https://www.sciencedirect.com/science/article/abs/pii/S0925231220305506

Trouvain, N., Pedrelli, L., Dinh, T. T., & Hinaut, X. (2020). Reservoirpy: An efficient and user-friendly library to design Echo State Networks. *Artificial Neural Networks and Machine Learning – ICANN 2020*, 494–505. https://doi.org/10.1007/978-3-030-61616-8_40

Verzelli, P., Alippi, C., & Livi, L. (2019, September 25). *Echo State Networks with self-normalizing activations on the hyper-sphere*. Nature News. Retrieved from https://www.nature.com/articles/s41598-019-50158-4

Wolchover, N. (2018, April 18). *Machine Learning's 'amazing' ability to predict chaos*. Quanta Magazine. Retrieved from https://www.quantamagazine.org/machine-learnings-amazing-ability-to-predict-chaos-20180418/

Wu, H., Chen, Z., Sun, W., Zheng, B., & Wang, W. (2017, August). *Modeling trajectories with recurrent neural networks*. Retrieved from https://www.ijcai.org/Proceedings/2017/0430.pdf

Ying, X. (2019). *An overview of overfitting and its solutions*. IOPScience. Retrieved from https://iopscience.iop.org/article/10.1088/1742-6596/1168/2/022022

Zaremba, W., Sutskever, I., & Vinyals, O. (2015, February 19). *Recurrent neural network regularization*. arXiv.org. Retrieved from https://arxiv.org/abs/1409.2329